

---

# ANALYSING THE CAUSES OF THE CHANGES IN AIRBORNE NO<sub>2</sub> AND CO EMISSIONS IN EUROPE DURING COVID-19 CRISIS

---

Bashini Mahaarachchi

University of Potsdam  
*mahaarachchi@uni-potsdam.de*  
Matriculation No: 800190

December 2, 2020

## ABSTRACT

Due to the contagion of COVID-19 governments across the world imposed travel restrictions and locked down several cities. As a result human mobility and related activities declined significantly until the bans were lifted. The decline in activities that demanded high level of energy consumption resulted with significant reduction in air pollution in many regions. This sharp drop in air pollution in several countries and regions was captured by satellite images [2, 10]. In this study, the relationships of airborne CO and NO<sub>2</sub> emissions (acquired by SENTINEL-5 satellite observations) with population, road traffic and vessel traffic in Europe are investigated. Results confirm that road traffic has been the primary reason for the reduction in NO<sub>2</sub> emissions during the lock-down period.

**Keywords** Covid-19 · Europe · NO<sub>2</sub> emission · CO emission · road traffic · population · marine/vessel traffic.

## 1 INTRODUCTION

The emergence of COVID-19 was declared a global pandemic by the World Health Organization on 11 March 2020. Cases rapidly spread, initially in China during January, quickly expanding to South Korea, Japan, Europe (mainly Italy, France and Spain) and the United States in late January [22].

Following the spread of the virus, to contain it, strict measures were put in place by governments as an effort to isolate cases and stop the transmission of the virus. The measures imposed ranged from the quarantining of symptomatic individuals to banning of mass gatherings, mandatory closure of schools/universities, mandatory home confinement and banning of border crossings. These confinement measures led to drastic changes in energy use, with expected reduction in pollutant emissions.

This study investigates if the reduction in human activities and vehicle movement occurred due to confinement measures have influenced the changes in airborne CO and NO<sub>2</sub> emissions. The main goal of this study is to see if there is a noticeable relationship between emission levels and road traffic, population and vessel traffic data. This study extends some of my previous work, used to analyse CO and NO<sub>2</sub> emission levels in Europe and population density in European countries [15].

In this analysis the time between **1<sup>st</sup> of March 2020 to 31<sup>st</sup> of April 2020** is considered as the time where strict confinement policies were applied across Europe, thus the '**lock-down period**'. Furthermore, the number of roads that lie within a certain radius from each geographical location (road density) is considered as a surrogate to the road traffic levels, and similarly, number of vessel routes as a surrogate to vessel traffic in the Mediterranean Sea and the Black Sea.

## 2 LITERATURE REVIEW

### 2.1 Pollutant emissions, CO and NO<sub>2</sub>

Air pollutants can be classified as primary or secondary air pollutants. A primary pollutant is emitted directly from a source to the atmosphere, while secondary pollutants in the atmosphere are precursors of other pollutants (mostly primary) through reactions. An examples of a secondary pollutant include ozone, which is formed when hydrocarbons (HC) and nitrogen oxides (NO<sub>x</sub>) combine in the presence of sunlight. Another two examples for secondary air pollutant are NO<sub>2</sub>, which is formed when NO combines with oxygen in the air and acid rain, which is formed when sulphur dioxide or nitrogen oxides react with water [11].

Main primary air pollutants include particulate matter (PM), black carbon (BC), sulphur oxides (SO<sub>x</sub>), NO<sub>x</sub> (which includes both NO and NO<sub>2</sub>), NH<sub>3</sub>, CO, methane (CH<sub>4</sub>), non-methane volatile organic compounds (NMVOCs) including C<sub>6</sub>H<sub>6</sub>, certain metals and polycyclic aromatic hydrocarbons (PAH, including benzo[ $\alpha$ ]pyrene BaP) [19].

Main secondary air pollutants are PM (formed in the atmosphere), O<sub>3</sub>, NO<sub>2</sub> and a number of oxidised VOCs. Key precursor gases for secondary PM are SO<sub>2</sub>, NO<sub>x</sub>, NH<sub>3</sub> and volatile organic compounds (VOCs). The gases NH<sub>3</sub>, SO<sub>2</sub> and NO<sub>x</sub> react in the atmosphere to form NH<sub>4</sub><sup>+</sup>, SO<sub>4</sub><sup>2-</sup> and NO<sub>3</sub><sup>-</sup> compounds. These compounds form new particles in the air or condense onto pre-existing ones to form secondary PM (also called secondary inorganic aerosols) [19].

Carbon monoxide (CO) is produced in the incomplete combustion of carbon containing fuels such as gasoline, natural gas, oil, coal, and wood. The largest anthropogenic source of CO is vehicle emissions whilst the second largest proportion is coming from fuel combustion in boilers and incinerators as well as from household appliances fuelled with gas, oil, kerosene or wood [28].

The main source of nitrogen dioxide (NO<sub>2</sub>) is the combustion of fossil fuels (coal, gas and oil) especially fuel used in cars. It is also produced from making of nitric acid, explosive welding, refining of petrol and metals, commercial manufacturing and food manufacturing [23]. NO<sub>2</sub> is also a component of indoor tobacco smoke [18].

### 2.2 Main air pollutants and their sources in Europe

EEA's Air Quality 2019 report [19] illustrates the total emissions of pollutants in the EU-28, indexed as a percentage of their value in the reference year 2000. There were larger reductions in the EU-28 than in the EEA-33 for CO, NH<sub>3</sub>, NMVOCs, NO<sub>x</sub>, primary PM with a diameter of 10 µm or less (PM<sub>10</sub>) and SO<sub>x</sub> (see Fig.2.1).

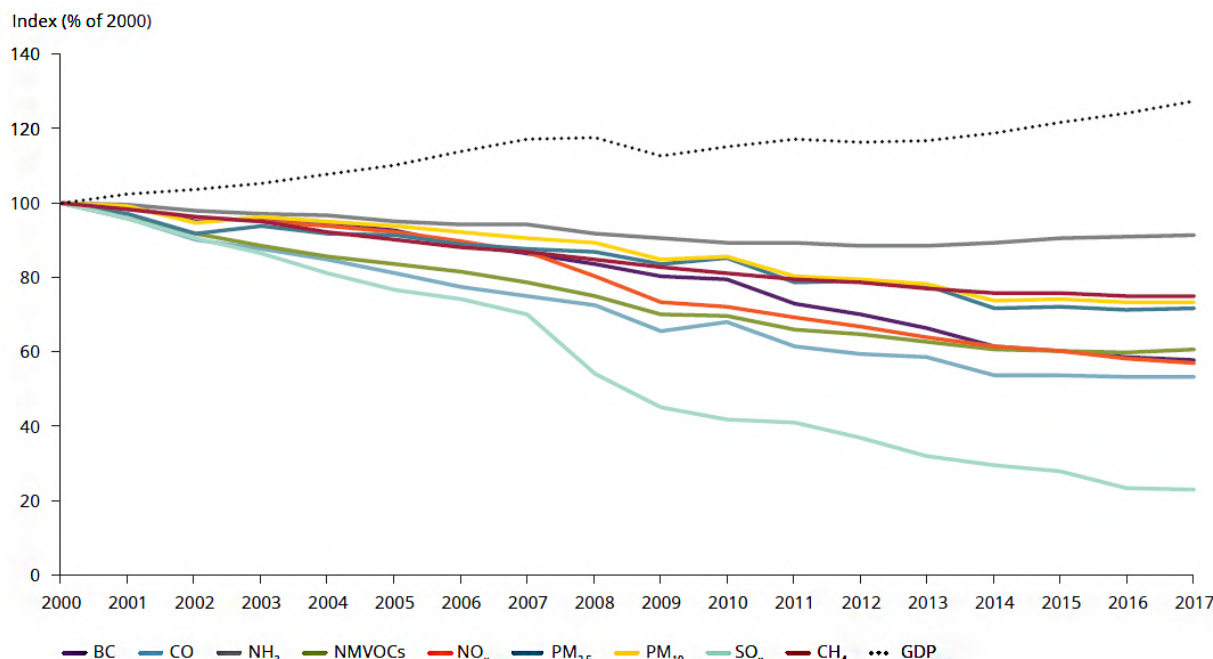


Figure 2.1: Trends in EU-28 emissions, 2000-2017 (as a % of 2000 levels): SO<sub>x</sub>, NO<sub>x</sub>, NH<sub>3</sub>, PM<sub>10</sub>, PM<sub>2.5</sub>, NMVOCs, CO, CH<sub>4</sub> and BC. Also for comparison EU-28 gross domestic product (GDP) is shown (GDP, expressed in chain linked volumes as a % of 2000 level).

During the period 2000–2017, emissions showed a significant absolute decoupling<sup>1</sup> from economic activity, which is desirable for both environmental and productivity gains. This is indicated by the contrast between a reduction in EU-28 air pollutant emissions and an increase in EU-28 GDP, which effectively means that there were fewer emissions for each unit of GDP produced per year consecutively. The greatest decoupling has been for SO<sub>x</sub>, CO, NO<sub>x</sub>, BC for which emissions per unit of GDP were reduced by over 40% between the years 2000 and 2017.

This report further gives an overview of each sector's contribution to total emissions for all chosen pollutants in the EU-28, for 2017 (see Fig. 2.2). The road transport sector was the most significant contributor to total NO<sub>x</sub>(nitrogen oxides is a generic term for the mono-nitrogen oxides NO and NO<sub>2</sub>) emissions and the second largest contributor for NO<sub>2</sub> emissions was energy production and distribution sector. The highest and the 50% contributor to total CO emissions was Commercial, institutional and households sector and second largest contributor to total CO emissions was transport sector [19].

The contributions from different emission source sectors to air pollutant concentrations and air pollution impacts depend not only on the amount of pollutants emitted but also on the proximity to the source, emission/dispersion conditions and other factors such as topography. Emission sectors with low emission heights, such as traffic and household emissions, generally make larger contributions to surface concentrations and health impacts in urban areas than emissions from high stacks.

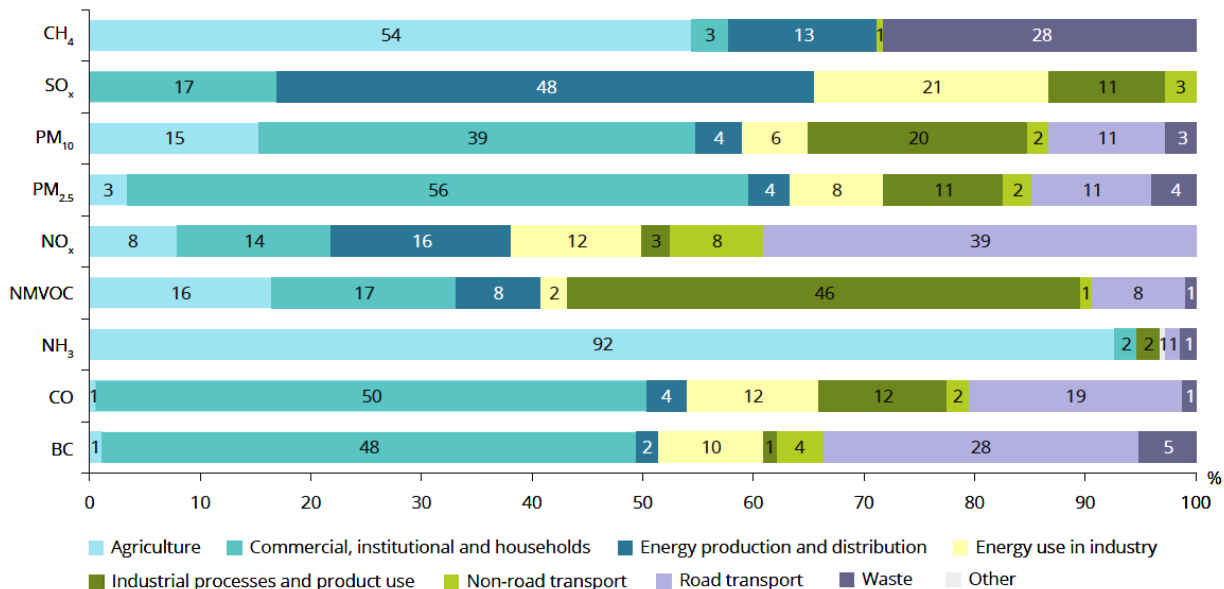


Figure 2.2: Contribution to EU-28 emissions from the main source sectors in 2017 of SO<sub>x</sub>, NO<sub>x</sub>, primary PM<sub>10</sub>, primary PM<sub>2.5</sub>, NH<sub>3</sub>, NMVOCs, CO, BC and CH<sub>4</sub> [19].

A study of European Environment Agency [1] states that from 1990 to 2017 emissions of nitrogen oxides decreased by 57% in European Economic Area (EEA) countries and 61% EU-28 countries (as also seen in Fig. 2.1). The main reason for this decline was the introduction of three-way catalytic converters in cars. However, the reduction of emissions from some modern vehicles have not met the initial expectations and the emission observed during the test-cycles of many of them exceeded the standards set for each of these vehicle type in Europe.

### 2.3 Changes in NO<sub>2</sub> and CO emissions during Covid-19 in Europe

According to the study of Quéré et al. (2020) the surface transport accounts for nearly half of the decrease in emissions during COVID-19 confinement and the daily global CO<sub>2</sub> emissions have reduced to 2006 levels during early April [14]. It further states that there was a 20% drop in power sector activities in Europe during COVID-19 lock-down period.

Data from the European Space Agency (ESA) show reductions in NO<sub>2</sub> concentrations from 13 March until 13 April 2020, compared to the March-April averaged concentrations from 2019 over Madrid, Milan and Rome around 45%, while in Paris a drastic reduction of 54%, coinciding with the strict quarantine measures implemented across Europe [3].

<sup>1</sup>'Absolute decoupling' is when a variable is stable or decreasing when the growth rate of the economic driving force is growing, while 'relative decoupling' is when the growth rate of the variable is positive but less than the growth rate of the economic variable.

The Mobilitaria report [12] states that the estimated reduction in traffic caused by lock-down in Italy is between 30% and 75%, with a corresponding reduction in emissions of NO<sub>2</sub> about 29% in March and 43% in April compared to the average for the same period from 2016 to 2019.

The most evident changes in UK air quality during lock-down have been in the urban environment, noticeably for NO<sub>x</sub>. The reductions in urban NO<sub>x</sub> averaged over the lock-down period is between 30% to 40%, with average NO<sub>2</sub> reductions of 20% to 30%. In general, NO<sub>x</sub> reductions have been greater at roadside than in urban background sites. These reductions would typically correspond to decreases in concentrations between 10 to 20  $\mu\text{gm}^{-3}$  when expressed relative to annual averages [13].

The study of Menut, L. et al., [17] show that the lock-down effect on atmospheric composition, in particular through massive traffic reductions, has affected several short-lived atmospheric trace species, with a large reduction in NO<sub>2</sub> concentrations, a lower reduction in PM concentrations and a mitigated effect on O<sub>3</sub> concentrations due to non-linear chemical effects.

### 3 METHODOLOGY

#### 3.1 Data sources

##### 3.1.1 Data for air pollutants

I used near real-time Level 3 processed NO<sub>2</sub> emission and CO emission data provided by TROPOMI-Sentinel-5 from European Union/ESA/Copernicus [5, 4], processed by and available in Google Earth Engine (GEE) [26, 25].

##### 3.1.2 Data for population

I used UN-Adjusted Population Density Data-Version 4.11 [20] to create population density maps, downloaded from GEE [9].

##### 3.1.3 Data for road network and vessel routes network

I downloaded the OpenStreetMap (OSM) Europe data extract in ‘.pbf’ format [7] and extracted the road network and the vessel routes network from it.

#### 3.2 Data processing steps

##### 3.2.1 Air pollutants data processing

Some of the steps relevant for this analysis were carried out in the previous study [15]. Following results of the previous study are used in this study.

7 by 7 kilometer resolution maps for the Europe region:

1. Percentage change of CO and NO<sub>2</sub> emissions during lock-down period compared to the average values of the previous year in the same period.
2. Slope of the time series change of CO and NO<sub>2</sub> emissions during lock-down period.

In addition to the previous results, maps that show: the mean NO<sub>2</sub> emission volumes during the lock-down period, during the previous two months and the same two maps for 2019 were created. Additional two maps that show the difference of mean CO emission between the two time periods were created since mean CO emission maps didn’t show a noticeable difference (see figures 4.4 and 4.5).

Furthermore, two video clips that show the weekly average change of NO<sub>2</sub> and CO emissions from 1<sup>st</sup> of January to 31<sup>st</sup> of August 2020 were created in GEE code editor. Please click on NO<sub>2</sub> and CO above to access the respective codes and please refer to section 4 for results.

To compare the results of the correlations (refer to section 3.2.5), more data was downloaded from GEE as GeoTIFF files. They were processed and relevant maps were created in python, as necessary.

### 3.2.2 Population data processing

The population density<sup>2</sup> map of Europe was also constructed as a 7 by 7 km resolution map. It shows the estimated number of persons per square kilometer in year 2020. This map was created using the same longitude and latitude points, considered for the air pollutant maps. This is also a result from the previous analysis [15] (see annex).

To compare the results of the correlations (refer to section 3.2.5), more data was downloaded from GEE as GeoTIFF files. They were processed and relevant maps were created in python, as necessary.

### 3.2.3 Road network data processing

The road density<sup>3</sup> map was constructed by calculating the number of roads that pass within a 7 km distance from the same longitude and latitude points considered in the air pollutant maps.

First the ‘.pbf’ file was clipped to 30 sub parts and then they were converted to GeoJSON files using OMS converter [8]. From each of the clipped files, the highways tagged as motorway, trunk, primary, secondary, tertiary, unclassified, and residential were selected. Then the results were saved as a .csv file keeping the ‘Osm id’ as the unique key, which distinguishes each road from one another.

Then the 30 datasets were merged in a way that the final dataset doesn’t have duplicated roads because of the clipping boundaries considered, i.e., part of a road segment can be in one clip and the other part can be in another clip. The duplicated ‘Osm id’ s were taken separately and the Linestring geometries of these duplicated ‘Osm id’s were merged. Finally, they were added back to the non-duplicated road dataset. The final dataset created has approximately 24 million unique roads in Europe (see Fig. 3.1).

Next, the road densities of geolocation points used to create the pollutant gas maps and population maps were calculated. The number of roads passing through 7 km radius from each of these points were calculated using Rtree spatial joins and spatial index, in python (see Fig. 4.2).

Processed road network dataset can be found [here](#).

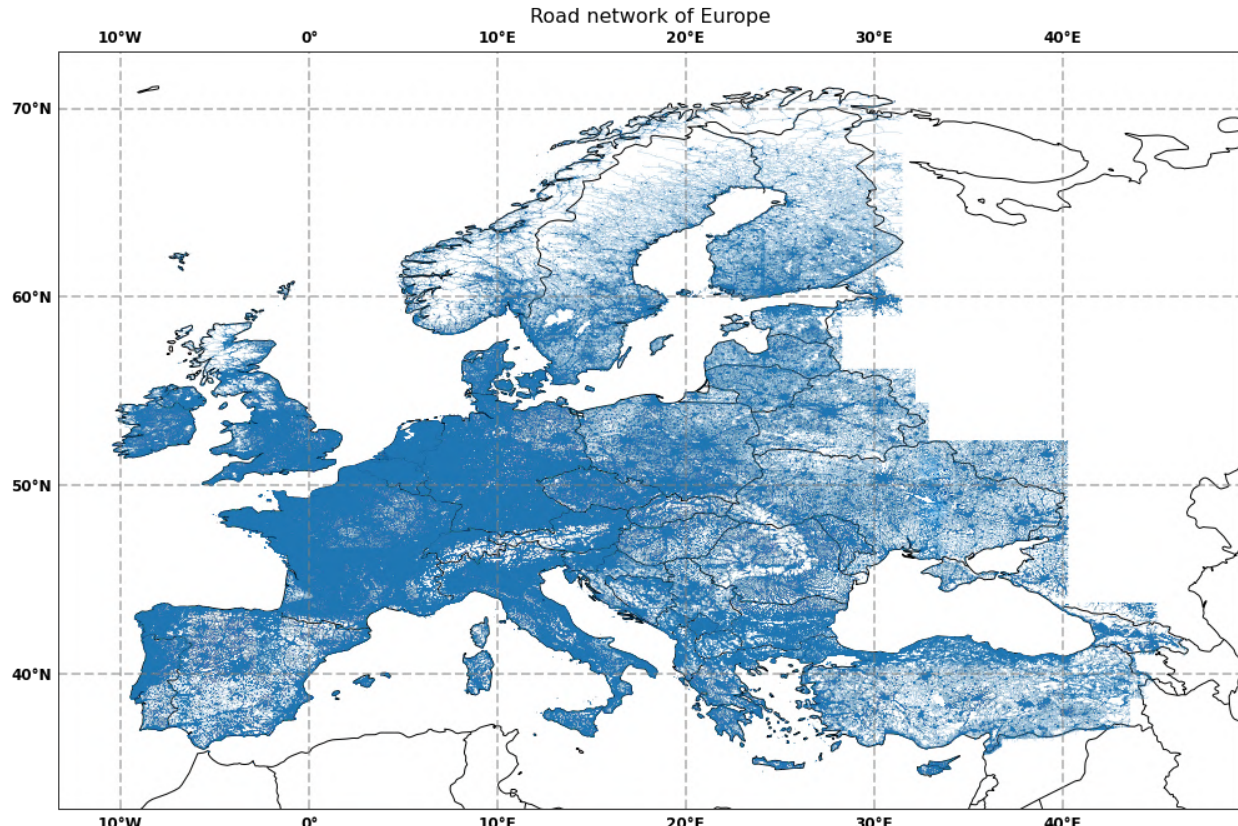


Figure 3.1: Road network of Europe extracted from OSM data; the highways tagged as motorway, trunk, primary, secondary, tertiary, unclassified, and residential in OSM.

<sup>2</sup>Population density (PD) refers to the number of persons within a 7 km radius from each of the considered geolocation.

<sup>3</sup>Road density (RD) refers to the number of roads pass within a 7 km radius from each of the considered geolocation.

### 3.2.4 Vessel network data processing

The method used to compute vessel densities<sup>4</sup> in the Mediterranean Sea and the black Sea is similar to the method used to compute road densities. The routes tagged as ‘ferry’ for ferry lines and ‘seamark:type’ equals to ‘separation\_boundary’ or ‘separation\_zone’ were selected to extract shipping lanes [27] from the OSM dataset (see Fig. 4.1).

The majority of vessel routes extracted from OSM are similar to the vessel routes available in marinetraffic.com [16]. Whereas some major shipping lines such as: Samsun-Turkey to Kerch-Russia, Novorossiysk-Russia and Tuapse-Russia are missing in OSM data (see Fig. 4.3).

### 3.2.5 Assessing the relationship between the air pollutant emissions, population, road traffic and vessel traffic

To assess the relationship of CO and NO<sub>2</sub> emission levels with the population, road traffic and vessel traffic, the Pearson’s correlation coefficient was calculated between the emission data and each of other variables. While doing the data pairs where the data is missing for one of the two variables were omitted (e.g., instances where for point A emission data is available but road density data is not available since there are no roads in 7 km radius surrounding point A). The results are shown in Table 4.1 and for relevant maps please refer to figures 4.6 to 4.20.

### 3.2.6 Assessing the relationship between the variables for subsets of dataset

According to the correlation statistics (see table 4.1), there are strong correlations between some of the variables. Subsets of data were selected (i.e., where PD is greater than 100, RD is greater than 250 and VD is greater than 1) to check if the correlation becomes stronger between the variables for the selected subsets of data (see table 4.2).

### 3.2.7 Time series analysis of emission levels

Surface traffic accounts for the largest part of the NO<sub>2</sub> emissions (see Fig. 2.2). Therefore, the top three geolocation points where RD and VD is high and the slope of NO<sub>2</sub> emission is also high were selected. Then the time series change of NO<sub>2</sub> volumes in these places were plotted (see Fig. 4.28 and 4.30).

Similarly, another three data points where PD is high, and the slope of CO emissions is also high were selected. Then the time series change of CO volumes in these places (see Fig. 4.29) were plotted. The geolocations with high PD were selected to plot time series change of CO emissions because the household sector accounts for the largest part of CO emissions (see Fig. 2.2).

GEE data has many emission data readings for a given geolocation for a given day. Therefore, the mean emission volume in each day of the selected geolocations were considered for the time series plots. Some of the data points were missing for NO<sub>2</sub> and many data points were missing for CO emissions. Therefore, the time series were smoothed with Savitzky–Golay filter [6].

## 4 RESULTS

Figure 4.1 shows the vessel lines density in the Mediterranean Sea and the Black Sea.

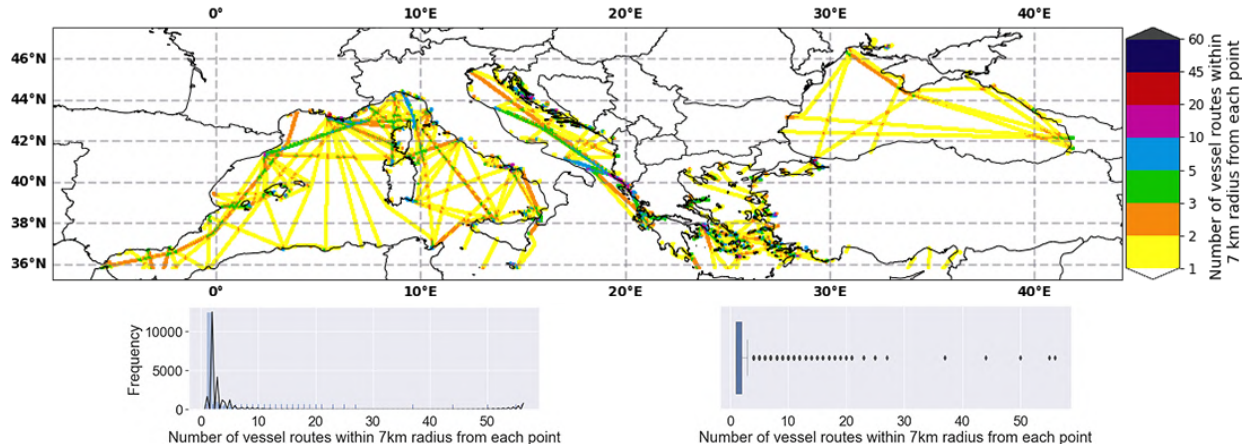


Figure 4.1: VD in the Mediterranean Sea and the Black Sea; number of vessel routes within a 7 km radius from each considered geolocation point. Each distinctive route is identified by a unique ‘Osm id’.

<sup>4</sup>Vessel density (VD) refers to the number of vessel routes within a 7 km radius from each of the considered geolocation.

## ANALYSING THE CAUSES OF THE CHANGES IN AIRBORNE NO<sub>2</sub> AND CO EMISSIONS IN EUROPE DURING COVID-19 CRISIS

---

Figure 4.2 shows the road density of Europe. Below the map the frequency distribution and the box plot of the number of roads are included.

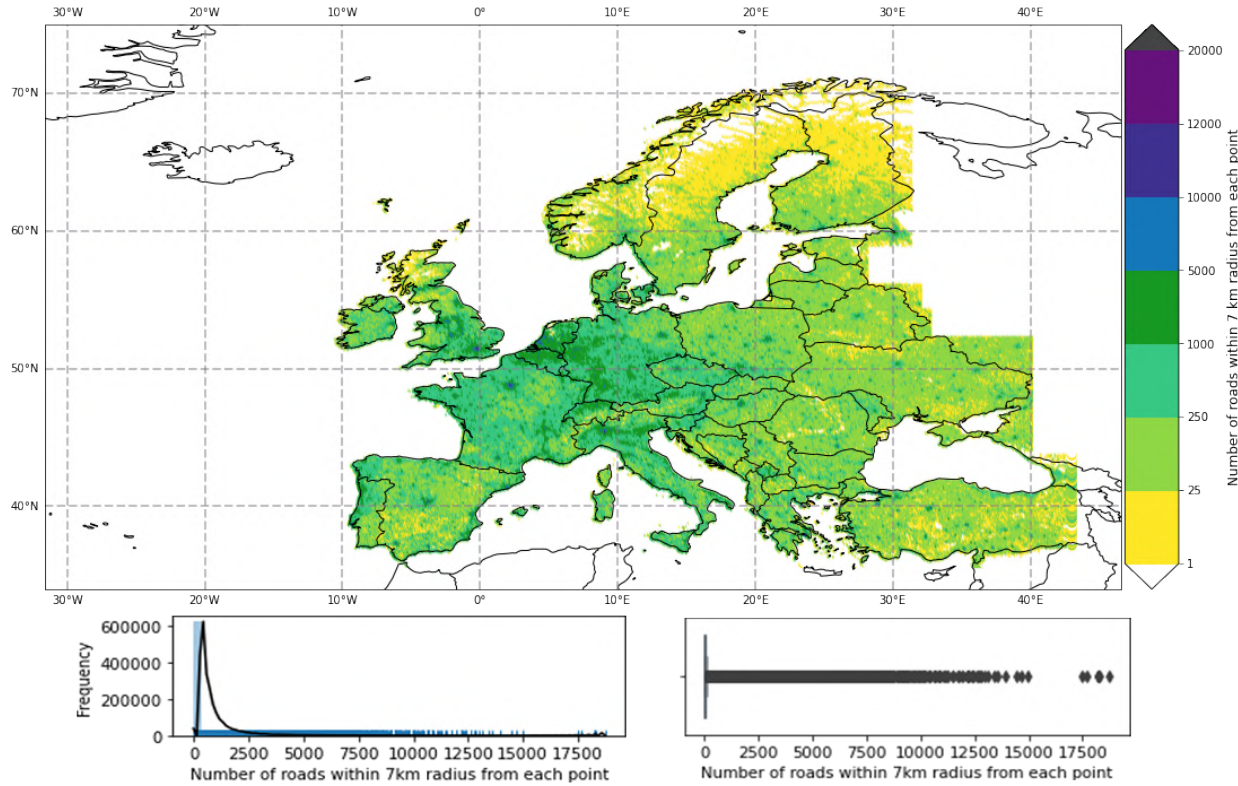


Figure 4.2: Road density of Europe; number of roads within a 7 km radius from each considered geolocation point. Each distinctive road is identified by a unique ‘Osm id’.

Figure 4.3 shows the vessel traffic density of the Mediterranean Sea and the Black Sea in marinetraffic.com on 09.10.2020. [16].

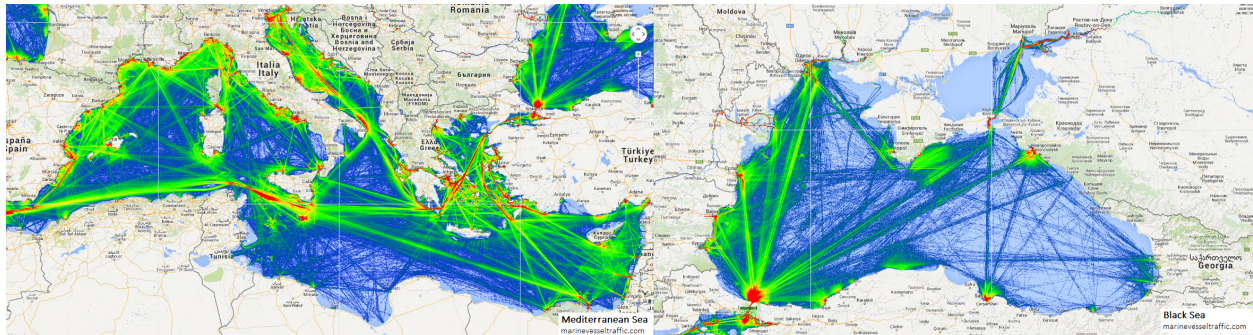


Figure 4.3: Vessel traffic density of the Mediterranean Sea and the Black Sea - Marinevesseltraffic.com [16].

The below hyperlinks include the video clips that show the weekly mean ( $\text{mol}/\text{m}^2$ ) of NO<sub>2</sub> and CO emissions from 1<sup>st</sup> of January to 31<sup>st</sup> July 2020.

1. NO<sub>2</sub> weekly average clip
2. CO weekly average clip

Figure 4.4 shows the mean NO<sub>2</sub> concentration in between ‘01-01-2020 to 29-02-2020’, ‘01-03-2019 to 30-04-2019’, ‘01-01-2020 to 29-02-2020’ and ‘01-03-2020 to 30-04-2020’. The two maps with the borders show the mean NO<sub>2</sub> emission volumes during the lock-down period. Similarly, figure 4.5 shows the mean CO concentration of the same periods. Last two maps in figure 4.5 show the difference of CO mean values ‘01-03-2019 to 30-04-2019’ minus ‘01-01-2020 to 28-02-2019’ and ‘01-03-2020 to 30-04-2020’ minus ‘01-01-2020 to 29-02-2020’.

## ANALYSING THE CAUSES OF THE CHANGES IN AIRBORNE NO<sub>2</sub> AND CO EMISSIONS IN EUROPE DURING COVID-19 CRISIS

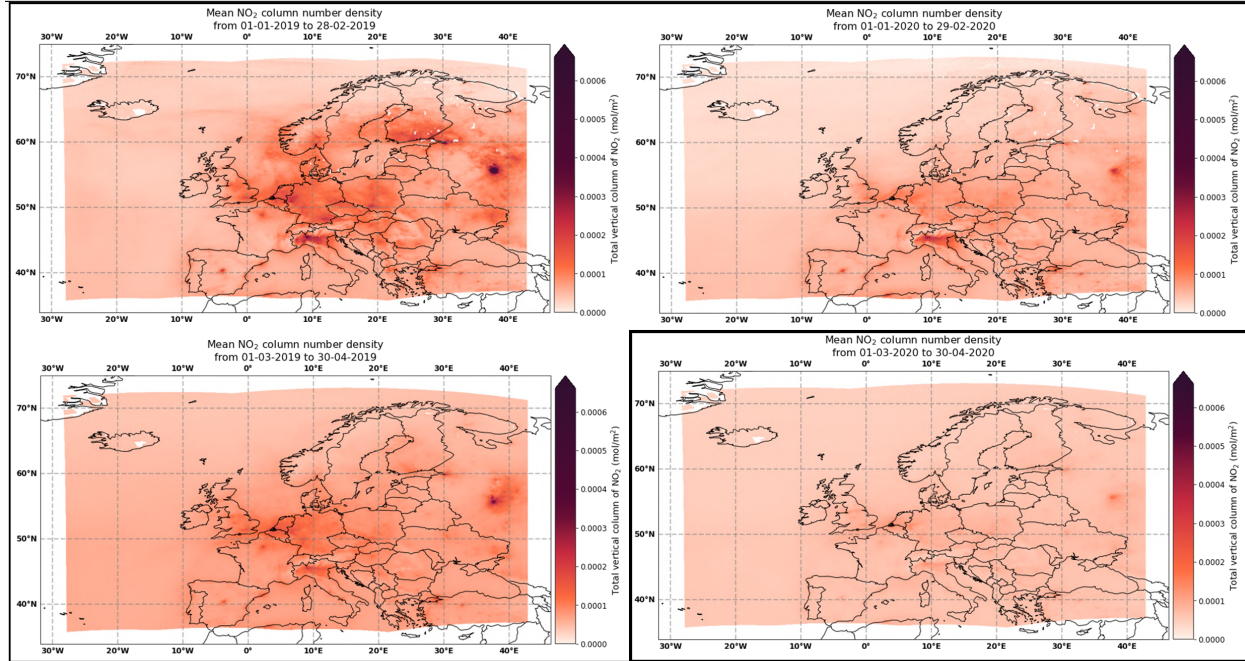


Figure 4.4: Mean NO<sub>2</sub> emission volumes during the lock-down period, during the previous two months and same maps for 2019 emissions.

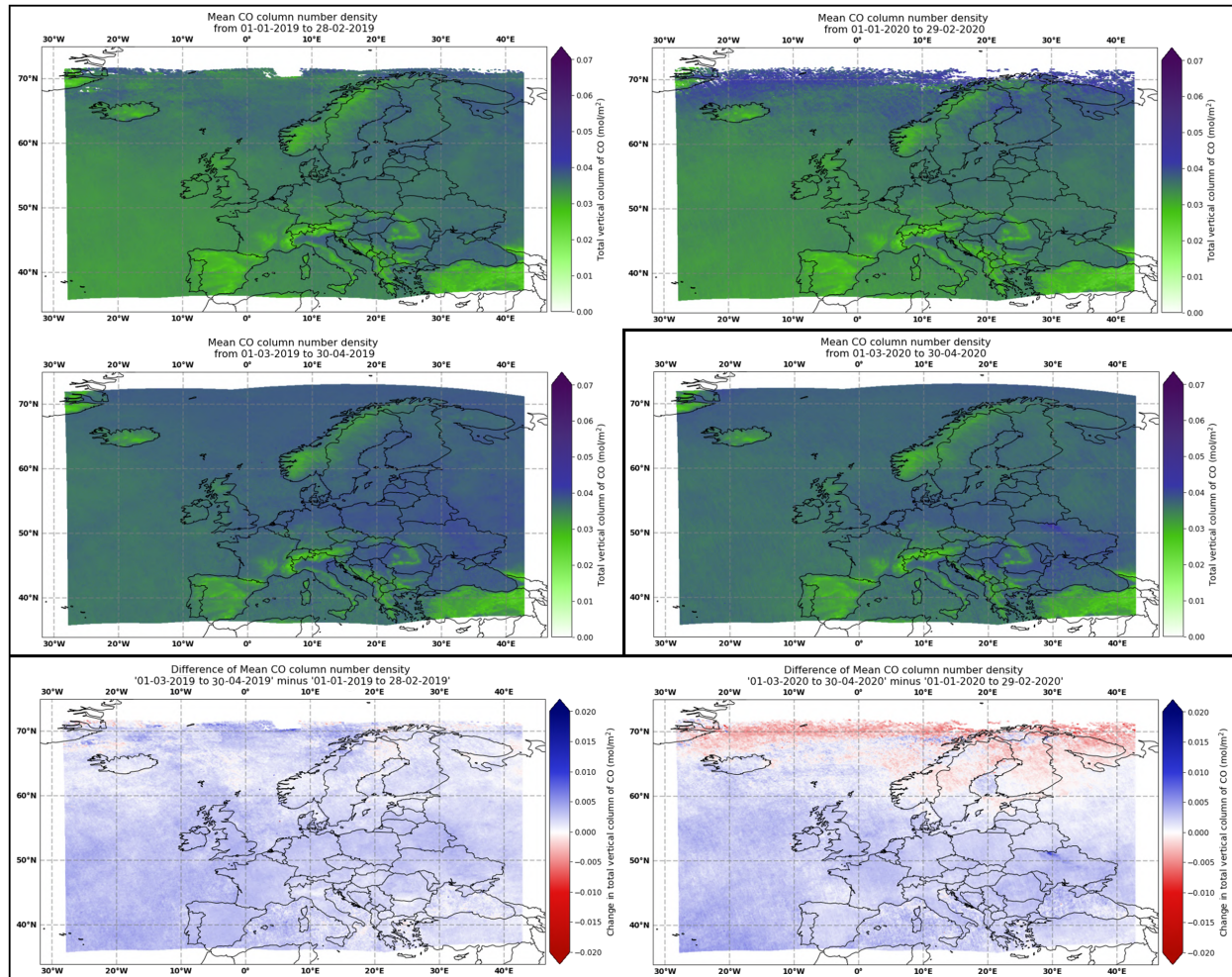


Figure 4.5: Mean CO emission volumes during the lock-down period, during the previous two months and same maps for 2019 emissions. Last two maps show the difference of CO mean values of the two periods in 2019 and 2020 respectively.

Table 4.1 shows the correlation statistics between the emission variables and the road density, vessel density and the population density.

Table 4.1: Correlation statistics between emission variables and RD, VD and PD. Mean CO and NO<sub>2</sub> are measured in mol/m<sup>2</sup> and road density and vessel density are measured in number of roads/number of vessel routes within a 7 km radius from each geolocation point. Population density is measured as the number of people living in 7 km radius from each geolocation point.

	Road density data		Vessel density data		Population density data	
	Correlation with road density data	p-value	Correlation with vessel density data	p-value	Corelation with population data	p-value
1 Slope of NO <sub>2</sub> gas volumes from 1st of March to 31st of April	-0.15	0.00	-0.09	3.32E-28	-0.11	0.00
2 Slope of CO gas volumes from 1st of March to 31st of April	0.05	1.24E-135	0.05	2.40E-09	0.06	6.08E-256
3 Mean NO <sub>2</sub> gas volumes from 1st of March to 31st of April	0.52	0.00	0.27	2.09E-238	0.35	0.00
4 Mean CO gas volumes from 1st of March to 31st of April	0.09	0.00	0.06	1.27E-11	0.07	5.98E-311
5 Percentage change of NO <sub>2</sub> gas volumes from 1st of March to 31st of April, compared to the seasonal values of 2019	-0.34	0.00	-0.11	1.65E-37	-0.16	0.00
6 Percentage change of CO gas volumes from 1st of March to 31st of April, compared to the seasonal values of 2019	0.07	2.73E-214	0.01	1.58E-01	-0.01	8.27E-09

Figures 4.6 to 4.20 show the pollutant emission data used to calculate the correlation statistics mentioned in table 4.1.

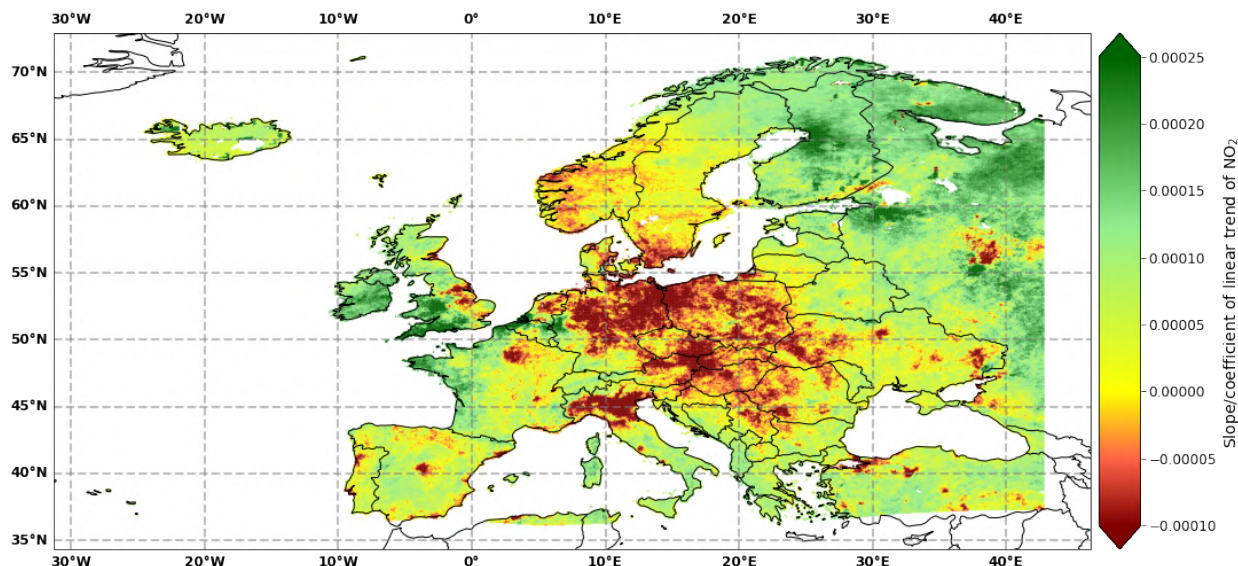


Figure 4.6: Slope of NO<sub>2</sub> emission data used to calculate the correlation between PD data and slope of NO<sub>2</sub> emission during the lock-down period. Negative slopes indicate reductions in NO<sub>2</sub> emission volumes and positive slopes indicate increases in NO<sub>2</sub> emission volumes.

ANALYSING THE CAUSES OF THE CHANGES IN AIRBORNE NO<sub>2</sub> AND CO EMISSIONS IN EUROPE  
DURING COVID-19 CRISIS

---

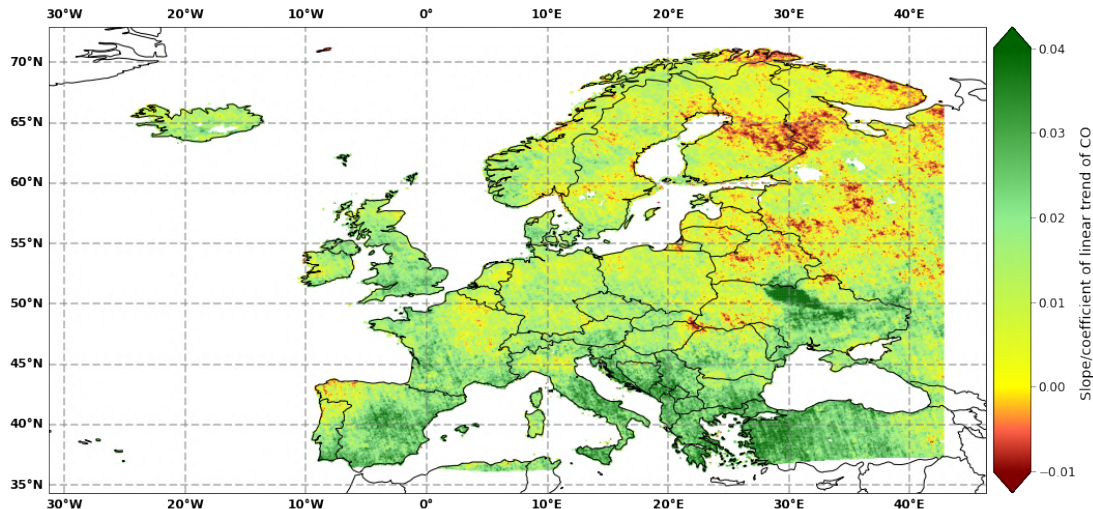


Figure 4.7: Slope of CO emission data used to calculate the correlation between PD data and slope of CO emission during the lock-down period. Negative slopes indicate reductions in CO emission volumes and positive slopes indicate increases in CO emission volumes.

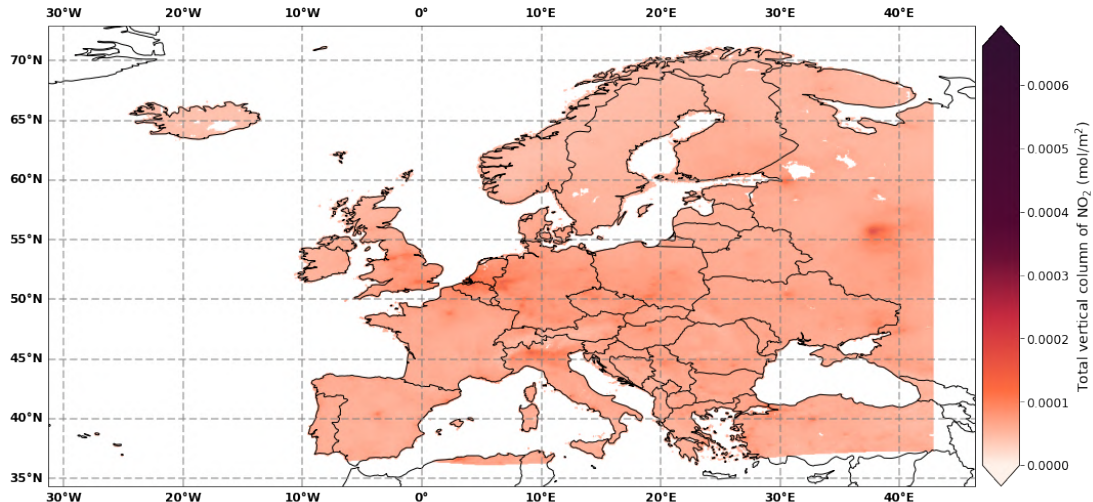


Figure 4.8: Mean NO<sub>2</sub> emission volume data used to calculate the correlation between PD data and Mean NO<sub>2</sub> emission volume during the lock-down period.

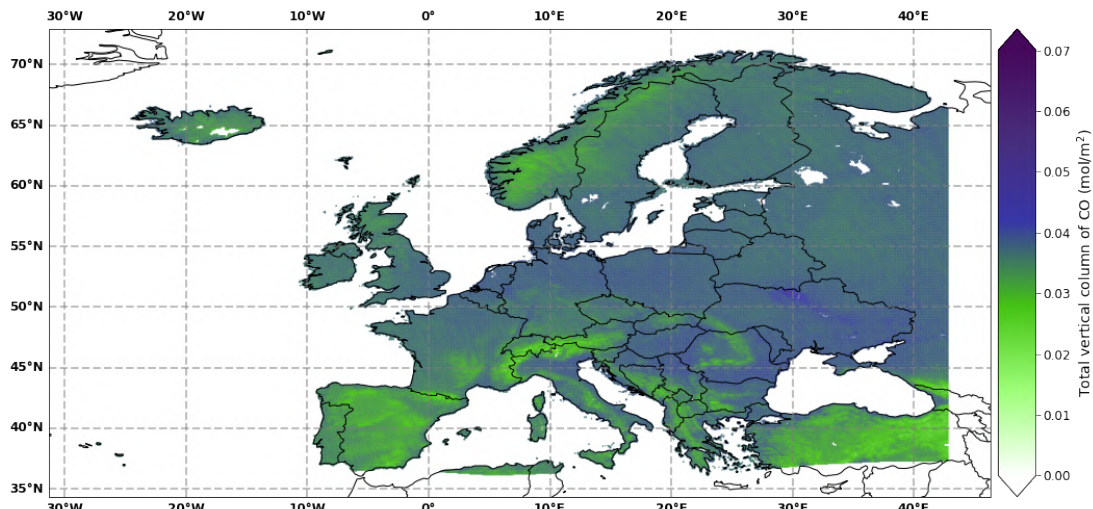


Figure 4.9: Mean CO emission volume data used to calculate the correlation between PD data and Mean CO emission volume during the lock-down period.

## ANALYSING THE CAUSES OF THE CHANGES IN AIRBORNE NO<sub>2</sub> AND CO EMISSIONS IN EUROPE DURING COVID-19 CRISIS

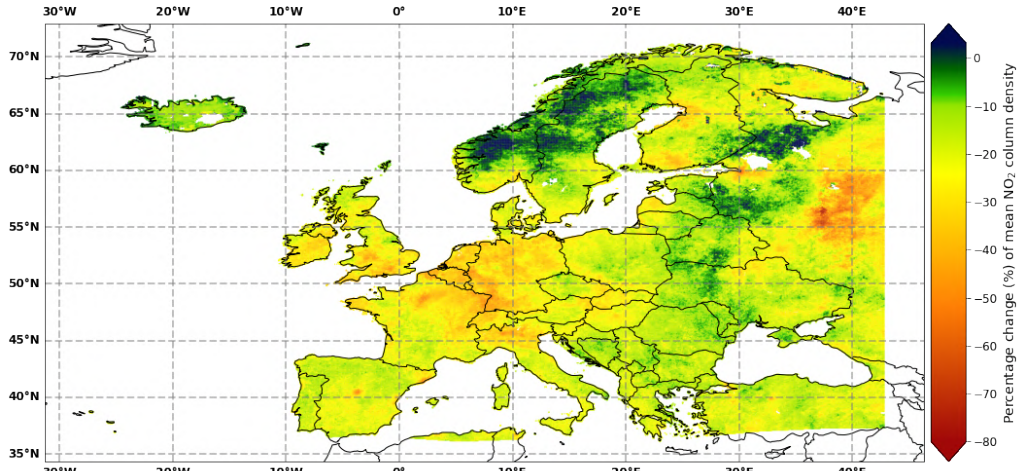


Figure 4.10: Percentage change of NO<sub>2</sub> emission volume data used to calculate the correlation between PD data and percentage change of NO<sub>2</sub> emission volume during the lock-down period. Percentages less than zero indicate reductions in NO<sub>2</sub> emission volumes and percentages greater than zero indicate increases in NO<sub>2</sub> emission volumes compared to the average values of the previous year in the same period.

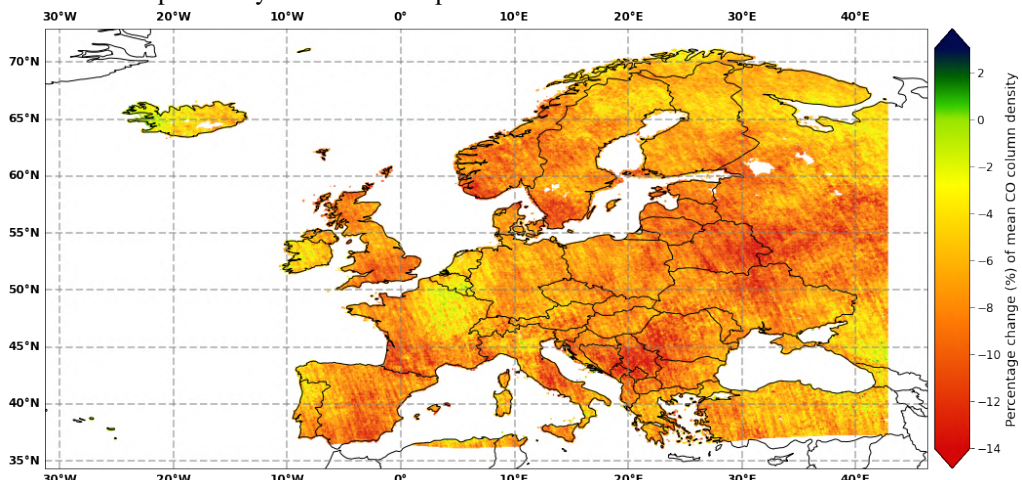


Figure 4.11: Percentage change of CO emission volume data used to calculate the correlation between PD data and percentage change of CO emission volume during the lock-down period. Percentages less than zero indicate reduction in CO emission volumes have decreased compared to the average values of the previous year in the same period.

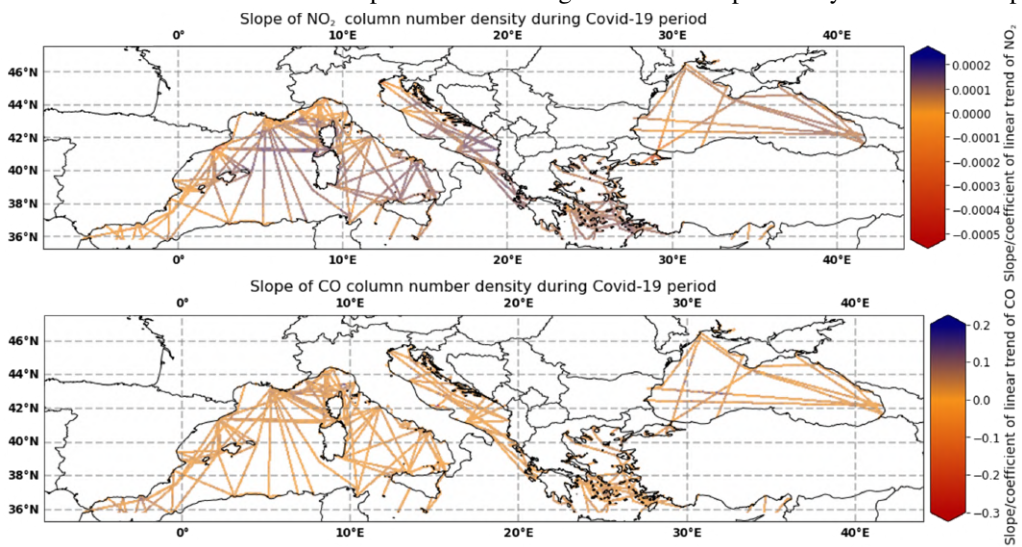


Figure 4.12: Slope of NO<sub>2</sub> emission and CO emission data used to calculate the correlation of VD and slope of NO<sub>2</sub> emission, and VD and slope of CO emission during the lock-down period. Negative slopes of NO<sub>2</sub> emission in the coastal areas in the Mediterranean Sea indicate reductions in NO<sub>2</sub> emission in this area.

ANALYSING THE CAUSES OF THE CHANGES IN AIRBORNE NO<sub>2</sub> AND CO EMISSIONS IN EUROPE  
DURING COVID-19 CRISIS

---

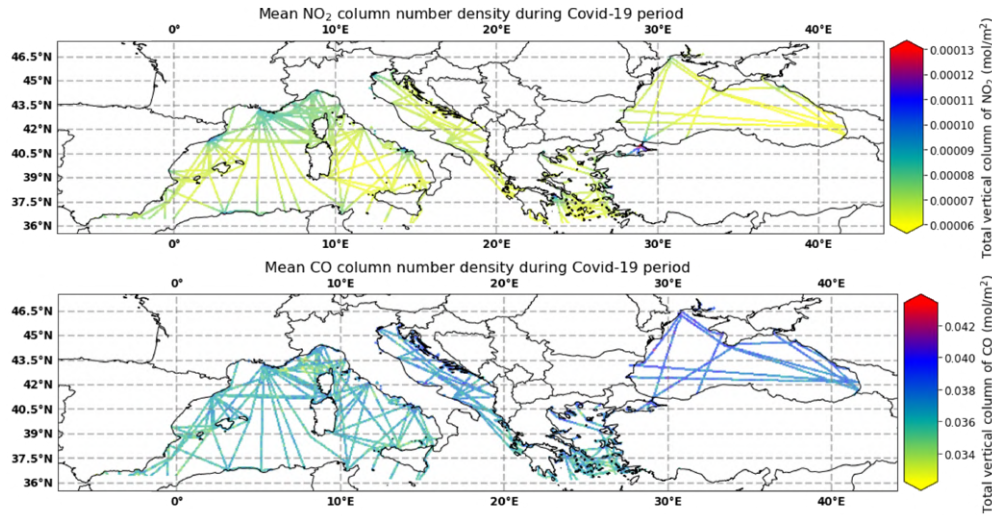


Figure 4.13: Mean NO<sub>2</sub> emission and CO emission data used to calculate the correlation of VD and mean NO<sub>2</sub> emission volume, and VD and mean CO emission volume during the lock-down period.

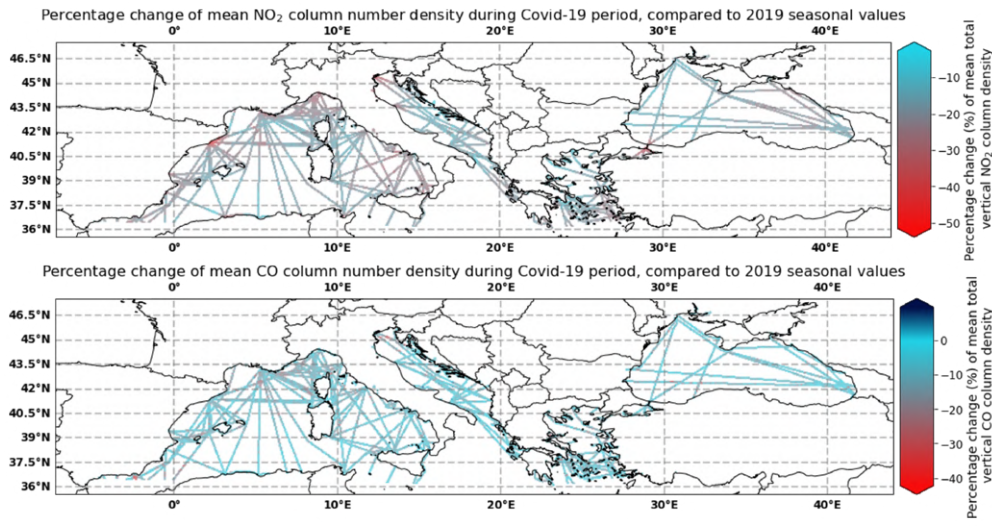


Figure 4.14: Percentage change of NO<sub>2</sub> emission and CO emission data used to calculate the correlation of VD and percentage change of NO<sub>2</sub> emission, and VD and percentage change of CO emission during the lock-down period.

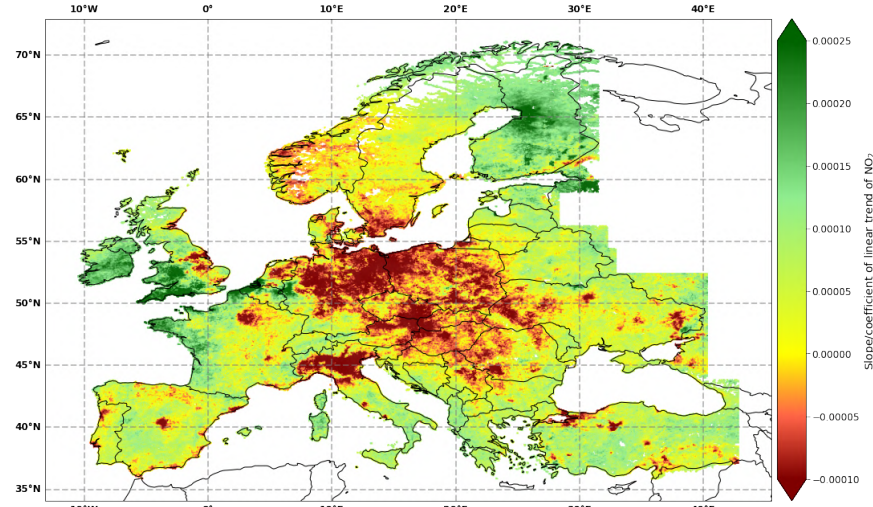


Figure 4.15: Slope of NO<sub>2</sub> emission data used to calculate the correlation between RD data and slope of NO<sub>2</sub> emission during the lock-down period. Negative slopes indicate reductions in NO<sub>2</sub> emission volumes and positive slopes indicate increases in NO<sub>2</sub> emission volumes.

ANALYSING THE CAUSES OF THE CHANGES IN AIRBORNE NO<sub>2</sub> AND CO EMISSIONS IN EUROPE  
DURING COVID-19 CRISIS

---

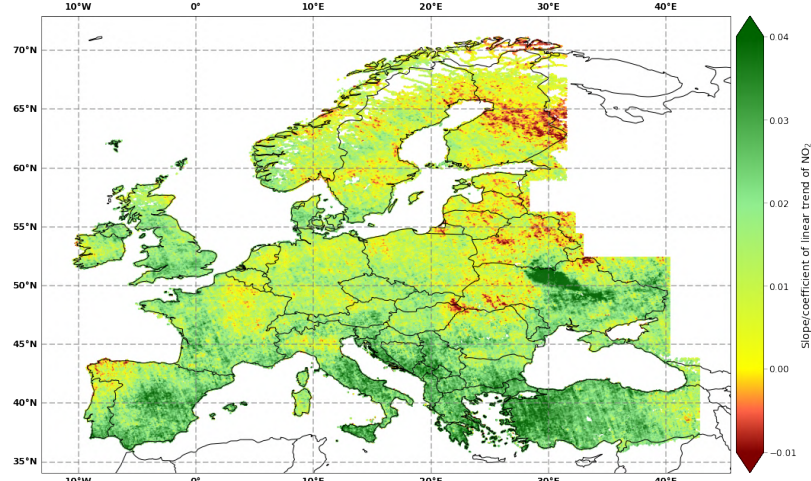


Figure 4.16: Slope of CO emission emission data used to calculate the correlation between RD data and slope of CO emission during the lock-down period. Negative slopes indicate reductions in CO emission volumes and positive slopes indicate increases in CO emission volumes.

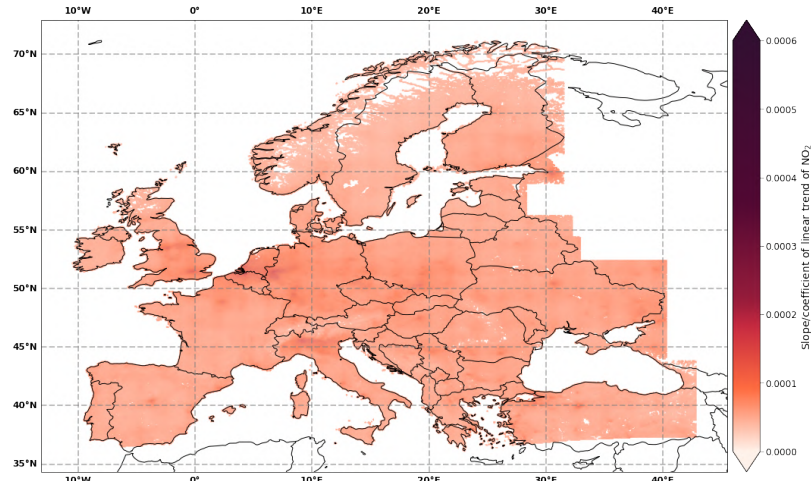


Figure 4.17: Mean NO<sub>2</sub> emission volume data used to calculate the correlation between RD data and Mean NO<sub>2</sub> emission volume during the lock-down period.

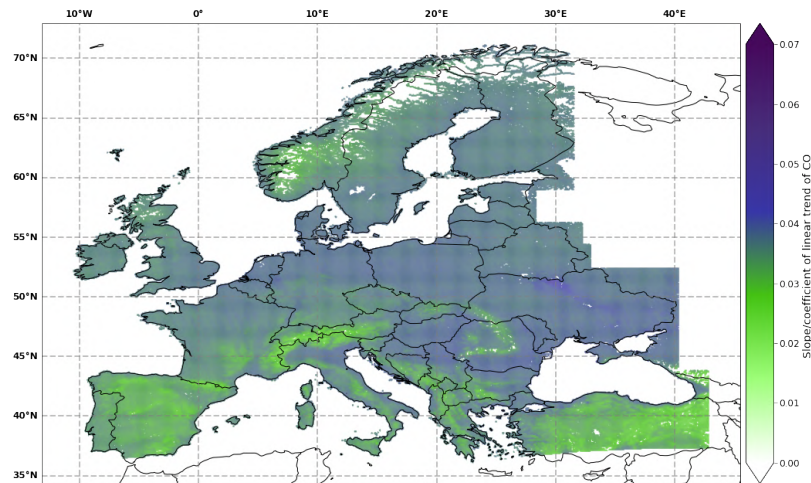


Figure 4.18: Mean CO emission volume data used to calculate the correlation between RD data and Mean CO emission volume during the lock-down period.

ANALYSING THE CAUSES OF THE CHANGES IN AIRBORNE NO<sub>2</sub> AND CO EMISSIONS IN EUROPE  
DURING COVID-19 CRISIS

---

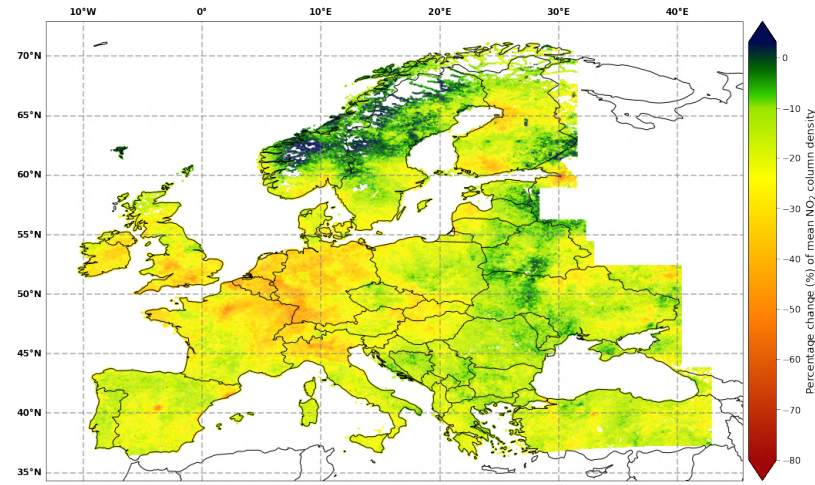


Figure 4.19: Percentage change of NO<sub>2</sub> emission volume data used to calculate the correlation between RD data and percentage change of NO<sub>2</sub> emission volume during the lock-down period. Percentages less than zero indicate reductions in NO<sub>2</sub> emission volumes and percentages greater than zero indicate increases in NO<sub>2</sub> emission volumes compared to the average values of the previous year in the same period.

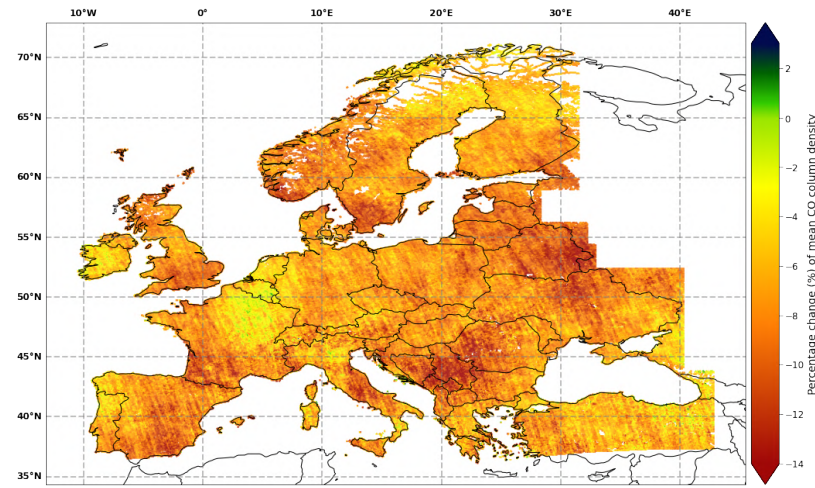


Figure 4.20: Percentage change of CO emission volume data used to calculate the correlation between RD data and Percentage change of CO emission volume during the lock-down period. Percentages less than zero indicate reductions in CO emission volumes and percentages greater than zero indicate increases in CO emission volumes compared to the average values of the previous year in the same period.

Correlation statistics of selected subsets of the dataset are shown in table 4.2.

Table 4.2: Correlation statistics calculated for subsets of dataset. Subsets are selected from the dataset where there was a strong correlation was observed between the variables initially (see Table 4.1). Conditions used for selecting subsets are mentioned in the table headings. If the correlation for subset becomes stronger than in the initial correlation, values are marked ↑ and if the correlation becomes weaker they are marked as ↓. Mean NO<sub>2</sub> are measured in mol/m<sup>2</sup> and road density and vessel density are measured in number of roads/number of vessel lines within a 7 km radius from each geolocation point. Population density is measured as the number of people living within a 7 km radius from each geolocation point.

	Road density data, where road density > 250 roads		Vessel density data, where vessel density >1		Population density data, where population densiy > 100	
	Correlation with road density data	p-value	Correlation with vessel density data	p-value	Corelation with population data	p-value
1 Mean NO <sub>2</sub> gas volumes from 1st of March to 31st of April	0.46	0.00	0.29	4.30E-98	0.31	0.00
2 Percentage change of NO <sub>2</sub> gas volumes from 1st of March to 31st of April, compared to the seasonal values of 2019	-0.24	0.00	N/A	N/A	N/A	N/A

## ANALYSING THE CAUSES OF THE CHANGES IN AIRBORNE NO<sub>2</sub> AND CO EMISSIONS IN EUROPE DURING COVID-19 CRISIS

---

Figures 4.21 to 4.23 show the pollutant emission data, RD, PD and VD data used to calculate the correlation statistics mentioned in table 4.2.

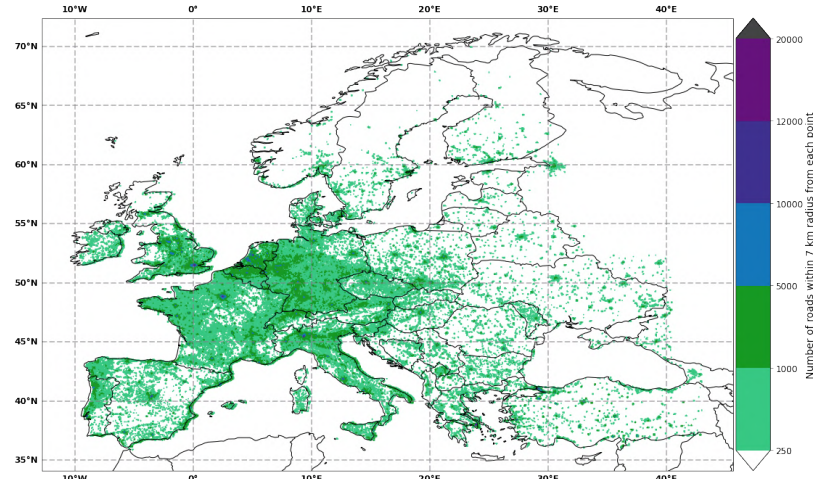


Figure 4.21: RD data used for calculating correlation statistics of percentage change of NO<sub>2</sub> emission volume and RD data, and Mean NO<sub>2</sub> emission volume data and RD data in places where RD > 250 (mentioned in Table.4.2).

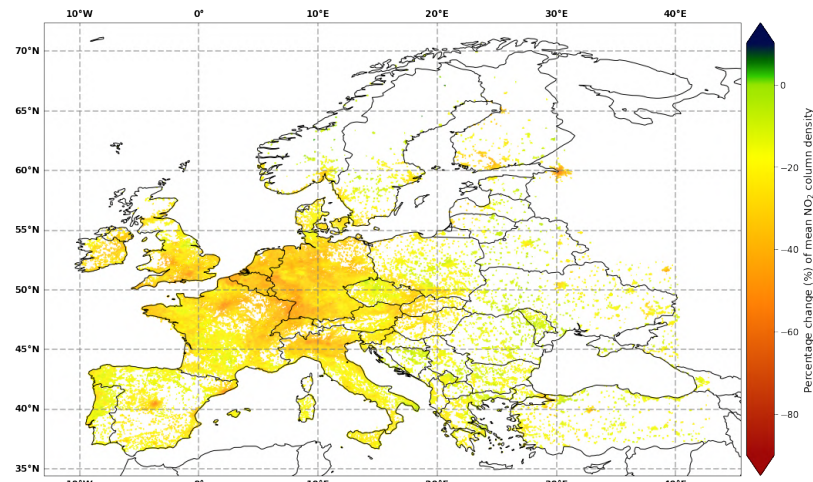


Figure 4.22: Percentage change of NO<sub>2</sub> emission volume data used for calculating correlation statistic between percentage change of NO<sub>2</sub> emission volume and RD data in places where RD > 250 (mentioned in Table.4.2).

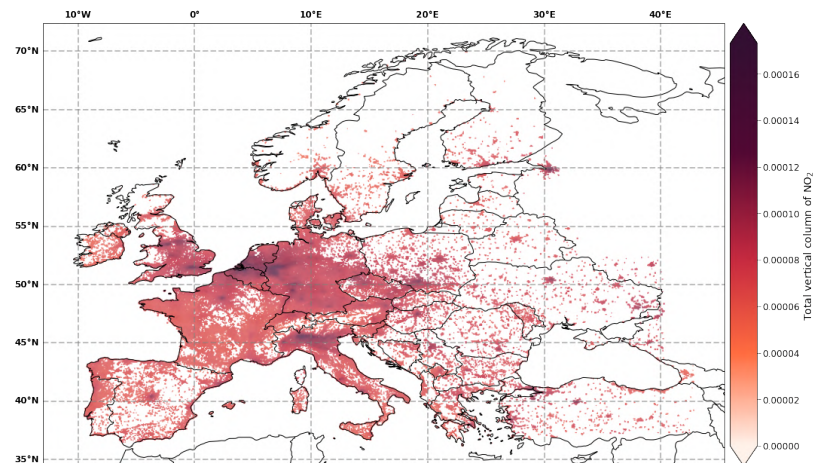


Figure 4.23: Mean NO<sub>2</sub> emission volume data used for calculating correlation statistics between mean NO<sub>2</sub> emission volume and RD data in places, where RD > 250 (mentioned in Table.4.2).

ANALYSING THE CAUSES OF THE CHANGES IN AIRBORNE NO<sub>2</sub> AND CO EMISSIONS IN EUROPE  
DURING COVID-19 CRISIS

---

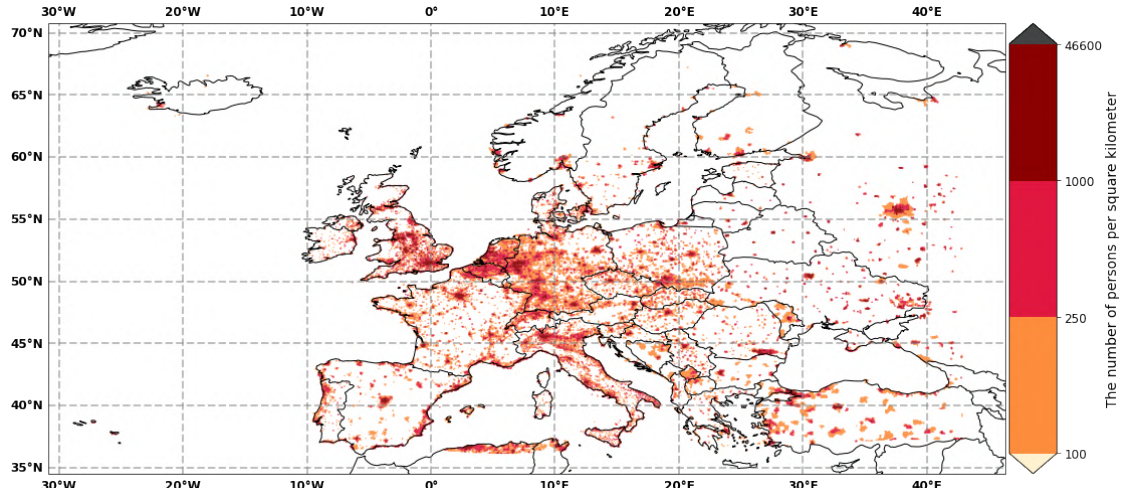


Figure 4.24: PD data used for calculating correlation statistic between mean NO<sub>2</sub> emission volume and PD, where PD > 100 (mentioned in Table.4.2).

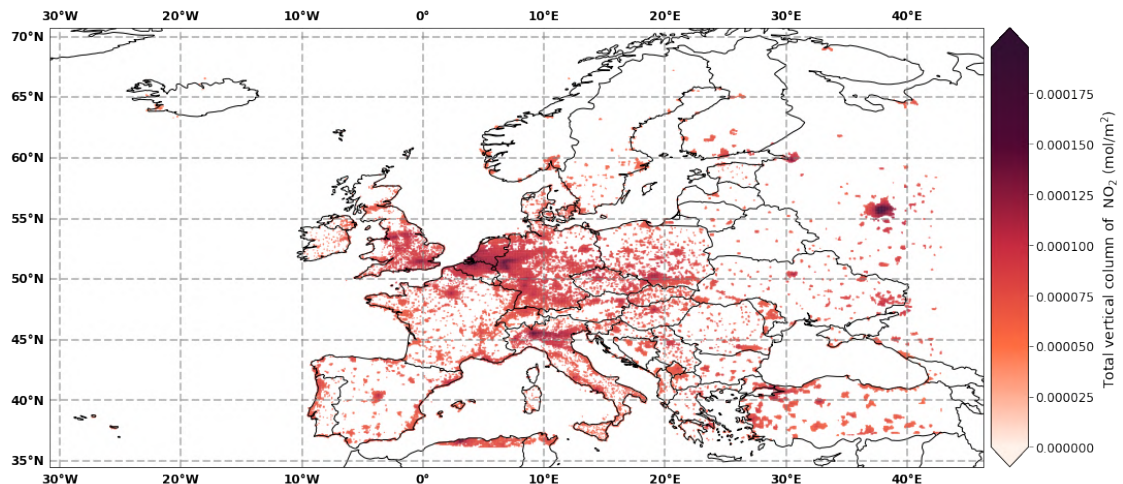


Figure 4.25: Mean NO<sub>2</sub> volume data used for calculating correlation statistic between mean NO<sub>2</sub> emission volume and PD, where PD > 100 (mentioned in Table.4.2).

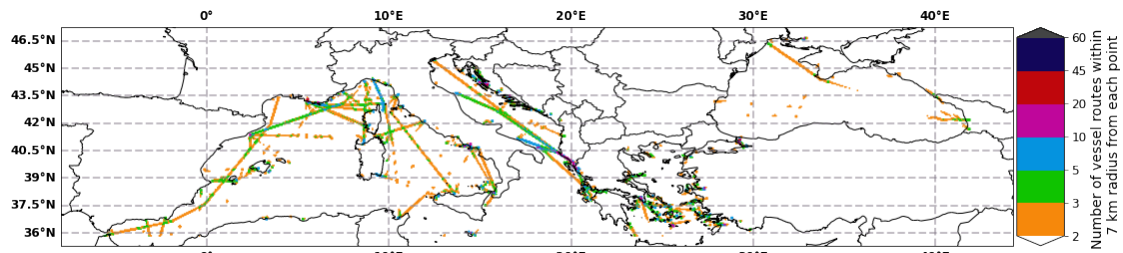


Figure 4.26: VD data used for calculating correlation statistic between Mean NO<sub>2</sub> volume and VD, where VD > 1 (mentioned in Table.4.2).

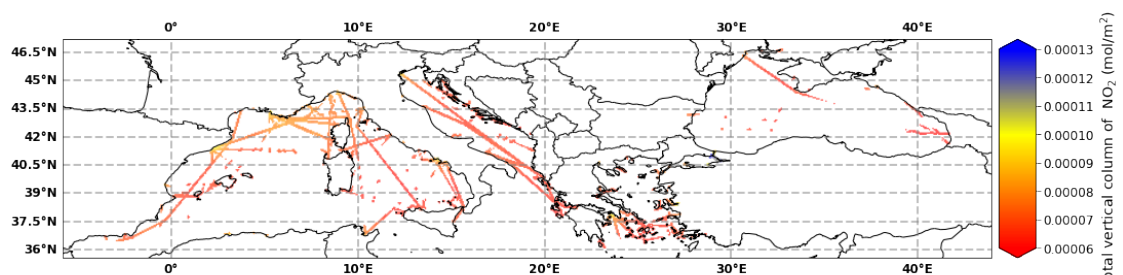


Figure 4.27: Mean NO<sub>2</sub> volume data used for calculating correlation statistic between Mean NO<sub>2</sub> volume and VD, where VD > 1 (mentioned in Table.4.2).

ANALYSING THE CAUSES OF THE CHANGES IN AIRBORNE NO<sub>2</sub> AND CO EMISSIONS IN EUROPE  
DURING COVID-19 CRISIS

---

Figures 4.28 to 4.30 show the time series change of mean emission volumes in each day for selected locations (selected in section 3.2.7) starting from 1<sup>st</sup> of January to 31st of July 2020.

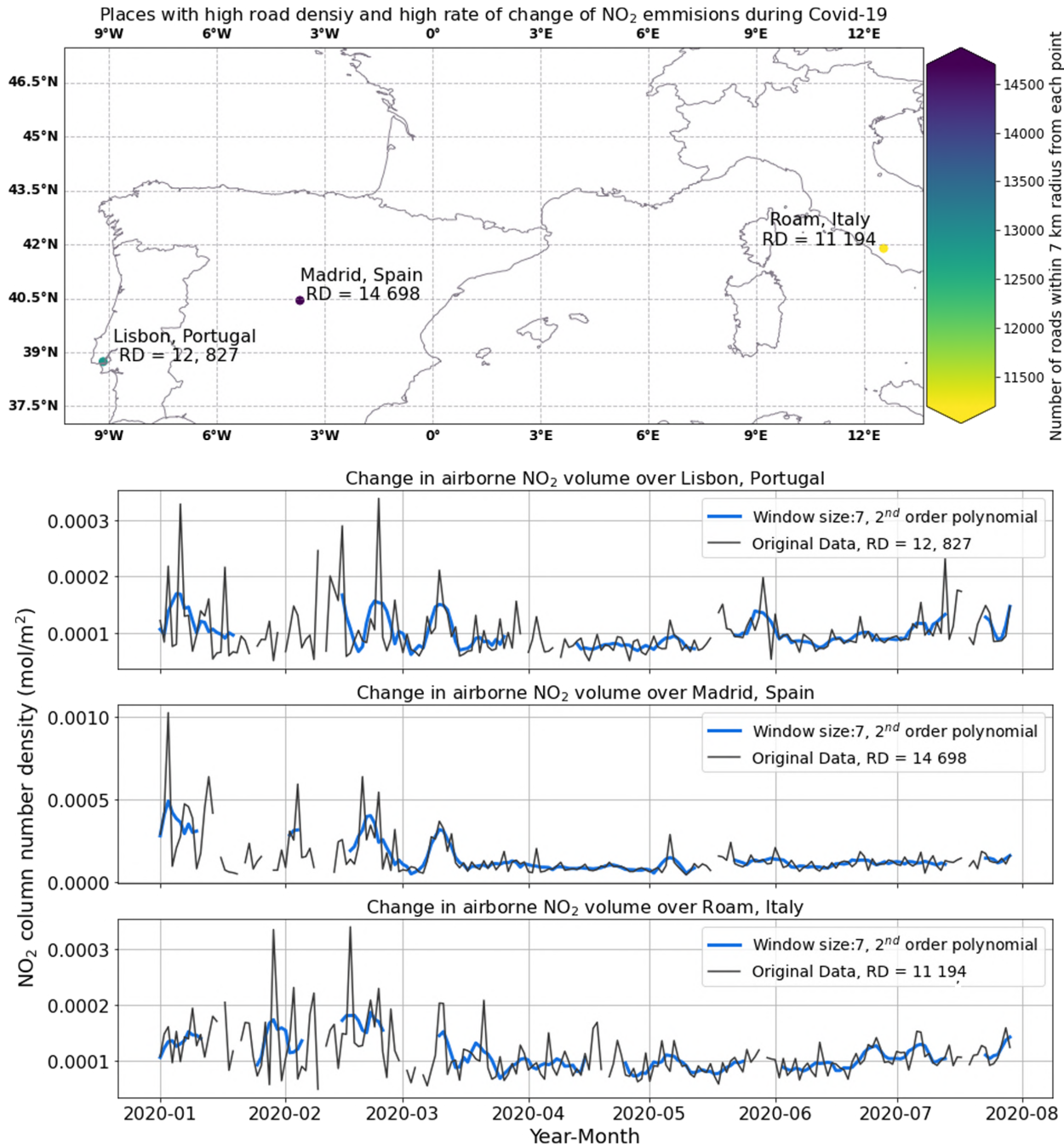


Figure 4.28: NO<sub>2</sub> emission time series change in Lisbon-Portugal, Madrid-Spain and Roam-Italy, and RD of these places. NO<sub>2</sub> emissions have dropped significantly during lock-down period in all these places. Volumes start to drop from mid March and start to increase again in late May.

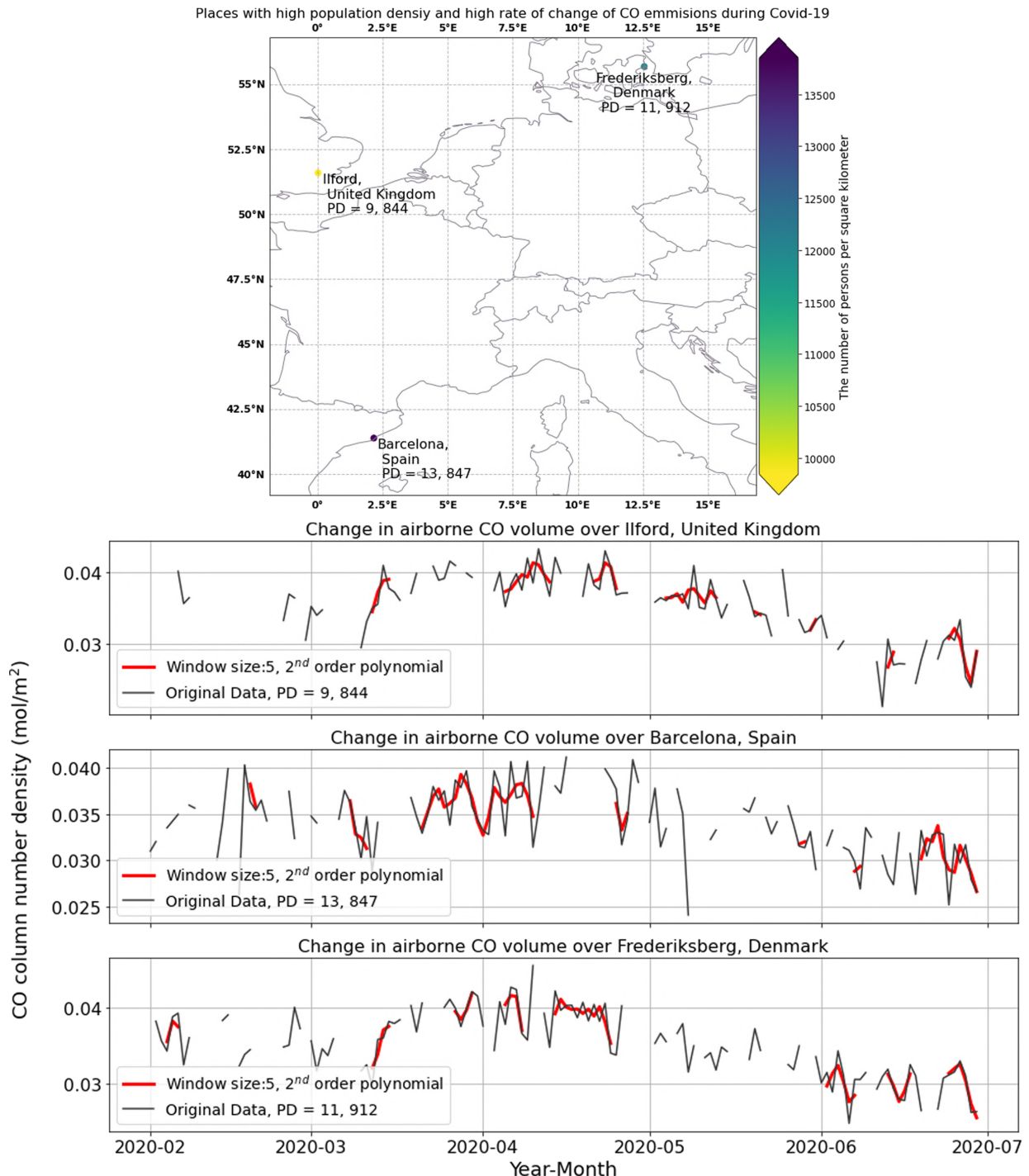


Figure 4.29: CO emission time series change and the smoothed series in Ilford-United Kingdom, Barcelona-Spain and Frederiksberg-Denmark, and PD of these places. CO emission has increased during the lock-down period in all these places. The emission volumes have started decreasing again from early May.

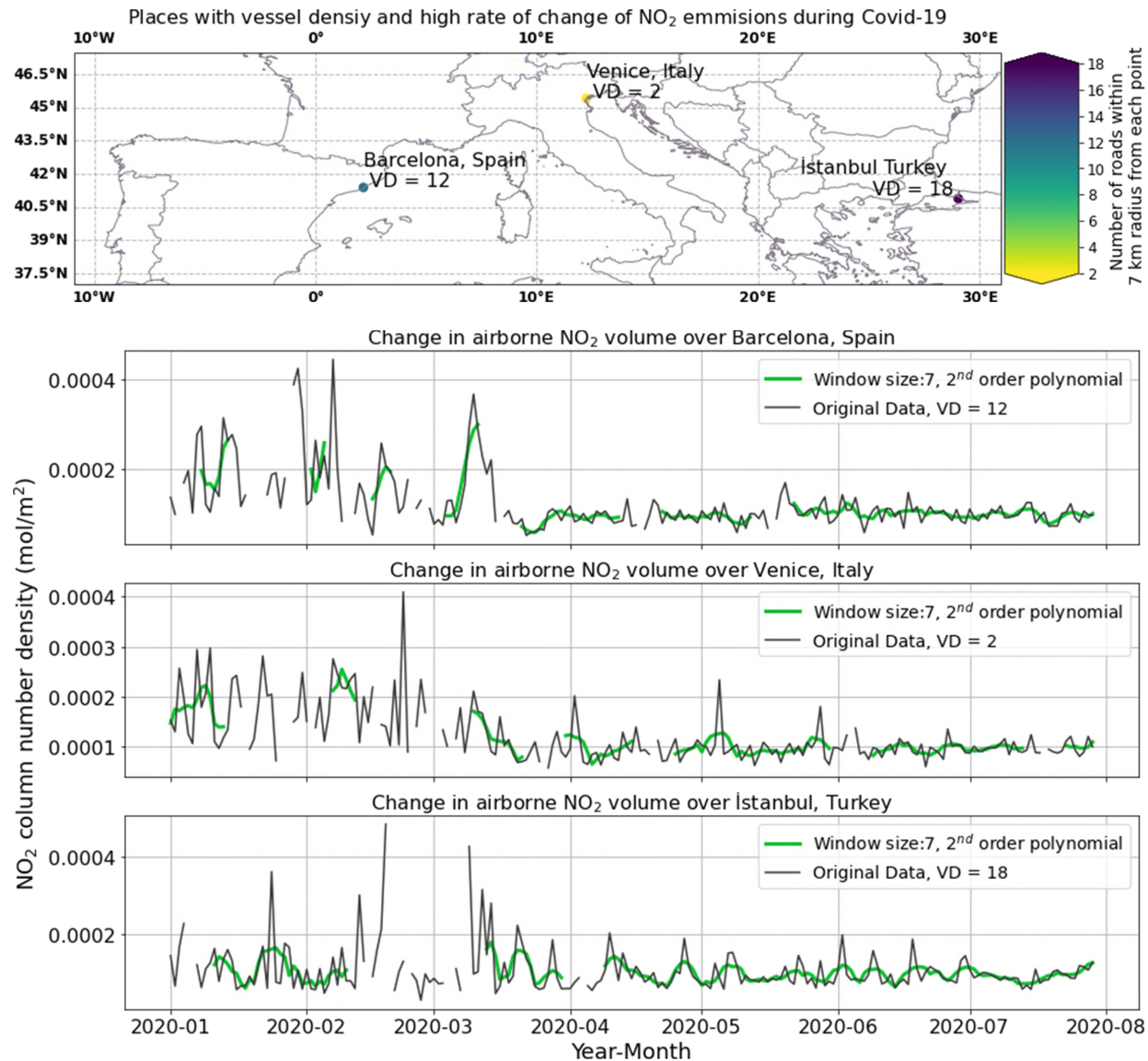


Figure 4.30: NO<sub>2</sub> emission time series and the smoothed series change in Barcelona-Spain, Venice-Italy and İstanbul-Turkey, and VD of these places. NO<sub>2</sub> emissions have dropped significantly during lock-down period in all these places. Similar to Fig.4.28, this drop has also started in mid March but it continues until the end of July with some irregular spikes in between.

## 5 DISCUSSION

### 5.1 Road density

Road density is in the range of 1,000-5,000 roads in most parts of West Germany, Netherlands, Belgium and Northern Italy. It is in the range of 5,000-10,000 roads in Madrid-Spain, Paris-France, Berlin-Germany, Prague-Czech Republic, Warsaw, Krakow and Poznan in Poland, Budapest-Hungary, Kiwi-Ukraine and Minsk-Belarus. Road density data contains some outlier values which are highly unlikely (e.g., above 15,000 roads within a 7 km radius).

This map goes inline with the percentage change of NO<sub>2</sub> emissions, slope of NO<sub>2</sub> emissions and the population density maps [15], which confirms the facts: 1) In the areas with higher level of human settlement there is a high level of road traffic, 2) Both population and road traffic largely contribute to the NO<sub>2</sub> emissions.

## 5.2 Vessel density

The Mediterranean Sea has highly dense vessel lines (5-10 vessel routes in 7 km radius) than the Black Sea. Among these vessel lines, the vessel lines, Barcelona-Spain to Genoa-Italy, Genoa-Italy to Bastia-France and Brindisi-Italy to Vlore-Albania are highlighted. From Vlore-Albania to Corfu Island-Greece and to Turkey there are some vessel densities that have 10-20 vessels routes with 7 km radius.

As mentioned in section 3.2.5, vessel density map is missing some major ship lines in the Black Sea. OSM data is widely used for street routing or navigation needs, but when it comes to marine navigation it may not have the correctly coded ‘Osm id’s and relevant information.

## 5.3 Correlation statistics and relationships

During Covid-19 confinement period NO<sub>2</sub> and CO emissions in Europe have dropped significantly, on average approximately 20% reduction of NO<sub>2</sub> and 7% reduction of CO emissions [15]. This is evident in figures 4.4 and 4.5. Mean NO<sub>2</sub> volume is higher in the 1<sup>st</sup> two months of the year than the mean of 3<sup>rd</sup> and 4<sup>th</sup> months in 2020 are lower. Whereas mean CO volume is lesser in 1<sup>st</sup> two months of the year than the mean of 3<sup>rd</sup> and 4<sup>th</sup> months. However, the observed changes in pollutant emissions could correspond to several possible factors:

1. A different meteorology from previous comparison period or years,
2. Decrease in anthropogenic emissions in Europe in every year (see Fig.2.1),
3. The current lock-down measures put in place to prevent the spread of Covid-19.

Therefore, it is difficult to calculate the contribution that correspond to the lock-down measures only.

Among the three candidate variables (RD, VD and PD), RD has the highest correlation with the pollutant gas variables. All three candidate variables have the highest correlation with the ‘Mean NO<sub>2</sub> volume’ compared to other emission variables.

‘Mean CO volume’ does not have a strong correlation with any of the candidate variables. Possible reason for this observation could be that the primary contributing source (accounts for 50%) of airborne CO in Europe is commercial, institutional and household sector as discussed in section 2.2. Road transport accounts only for 19% of the CO emissions. None of the three candidate variables capture the high contributing sectors of CO emissions except the little influence coming from the population density. CO is a highly dispersible gas [24], therefore, geo-dependent variables and CO emission measured at a specific location cannot be accurately compared. This could be the primary reason to have very weak correlation between ‘Mean CO volume’ and the candidate variables.

‘Percentage change of NO<sub>2</sub>’ has the next highest correlation to all three candidate variables and they are negative because as expected the NO<sub>2</sub> emissions are lower during the lock-down period than in the the previous year. In places where there is a high traffic density or a high population density, reduced NO<sub>2</sub> emission volumes are observed (see Fig.4.10).

‘Slope of NO<sub>2</sub> volume’ has the next highest correlation with the candidate variables and these correlation statistics are negative. ‘Slope of NO<sub>2</sub> volume’ and the three candidate variables together provide the best explanation for the reduction of NO<sub>2</sub> emissions during the lock-down period because the slope (coefficient of linear time series trend of air pollutants) during the lock-down period is a measurement that shows how rapidly the emission volumes have dropped during the lock-down.

Knowing that road transport accounts for 40% of the NO<sub>2</sub> emissions generally in Europe (see Fig. 2.2), it is realistic to observe a comparatively higher correlation value between ‘Slope of NO<sub>2</sub> volume’ and the RD than between ‘Slope of NO<sub>2</sub> volume’ and the PD. In general, high volumes of NO<sub>2</sub> are expected in places where there is a high RD and PD. Due to the confinement measures put in place during the lock-down period, vehicle movements and human activities have reduced in these places, which is the reason for having a high correlation between ‘Slope of NO<sub>2</sub> volume’ and RD, and ‘Slope of NO<sub>2</sub> volume’ and PD.

In contrast people staying at home due to the travel bans imposed could have contributed to higher level of CO emissions. CO can be emitted from fuel-burning appliances (water heaters, boilers, gas stoves, etc.) or any type of material burning at home. This could be the reason for ‘Slope of CO’ to have a very small but a highly significant and a positive correlation with the candidate variables while ‘Slope of NO<sub>2</sub>’ has a negative correlation with the candidate variables. ‘Percentage change of CO’ does not have a meaningful or significant relationships with any of the candidate variables, i.e., it has a negligible small positive correlation with RD but a negligible negative relationship with PD.

Correlation of RD with the emission volumes in the descending order is: ‘mean NO<sub>2</sub> volume’, ‘Percentage change of NO<sub>2</sub>’ and ‘Slope of NO<sub>2</sub>’. It is realistic to have a high correlation between RD and ‘mean NO<sub>2</sub> volume’ despite the

lock-down conditions because road traffic accounts for 40% of the total NO<sub>2</sub> emissions in Europe in general. Highly significant and strong negative correlations between the RD and ‘Percentage change of NO<sub>2</sub>’, and RD and ‘Slope of NO<sub>2</sub>’ confirm that road traffic reductions have largely contributed to the reduction in NO<sub>2</sub> emissions during the lock-down period.

The correlation of PD with the emission volume follows the same order as RD but not strong as the relationships between RD and emission variables. Stagnant areas with high human settlement contribute to high levels of indoor air pollution. ‘Commercial, institutional and households’ sector accounts for 14% of the NO<sub>2</sub> emissions and 50% of the CO emissions (see Fig. 2.2). PD has a stronger correlation with the NO<sub>2</sub> emissions than with the CO emissions which could be due to two facts: CO is a highly dispersing gas and from ‘Commercial, institutional and households’ sector emissions, largest contribution is coming from the ‘Commercial sector’.

VD also follows the same order of correlation patterns with the emission variables as RD and PD, but the correlation values are lower in magnitude. Reasons for this order of correlations is same as the reasons for the order of correlations between RD and emission variables. Study of RATA, V. et al., [21] identified maritime transport as the main factor of pollution in the Black Sea. Compared to classical terrestrial transport systems, it is more efficient in terms of energy efficiency, but NO<sub>x</sub>, SO<sub>2</sub> and PM emissions are much higher in the Black Sea due to a lack of regulation, the quality of fuels used for combustion and due to the sizing of the ships. The cease of ship transport during the lock-down period in the Black Sea and the Mediterranean Sea has resulted with lower emission levels in these two seas. This reduction was highlighted in the coastal areas of the Black sea and the Mediterranean Sea [15], where there is a high VD (see Fig. 4.1, 4.3, 4.12, 4.13 and 4.14).

The reason for VD to have comparatively weaker correlation statistics with emission variables than the RD could be the highly dense traffic routes in the Black Sea, which are unaccounted in this analysis as mentioned in section 5.2.

Furthermore, RD and VD are two proxy measures to the road traffic and vessel traffic; thus, they do not provide absolute measures to how changes in road traffic and vessel traffic during lock-down have affected the pollutant emission levels.

It would add further insights to this analysis if the locations of the industries that contribute to high level of NO<sub>2</sub> and CO emissions in Europe could be checked against the changes in CO and NO<sub>2</sub> emission levels in these locations during the lock-down period because 50% of the CO emissions and 8% of NO<sub>2</sub> emissions are coming from commercial institutions.

Taking subsets from the dataset to see if the relationship with emission variables becomes stronger in places where there is a high RD, PD or VD, has not resulted with stronger correlations except the correlation between VD and mean NO<sub>2</sub> volume during lock-down (see Fig.4.2), but this increase is also very small (increase of 0.02 in R value).

#### 5.4 Time series analysis of pollutant emission

Time series analyses done for CO and NO<sub>2</sub> emissions for selected places with high RD, PD and VD clearly show that:

1. NO<sub>2</sub> emissions have dropped significantly during lock-down period in the selected places with high RD. This drop is starting from mid March and starts to increase again in late May.
2. NO<sub>2</sub> emissions have dropped significantly during lock-down period in the selected places with high VD. Similar to the above scenario, this drop has also started in mid March but it continues until the end of July with some irregular spikes in between.
3. CO emission has increased during the lock-down period in the selected places with high PD. The emission volumes have started decreasing again from early May.

Despite the fact that these locations are in different countries and places in Europe, daily mean emission volumes in these places (for each scenario) follow the same pattern. CO emission has a lot of missing data during the entire considered time period.

## 6 CONCLUSIONS

Road traffic reduction has been the primary cause of reduction in NO<sub>2</sub> emissions during the lock-down period in Europe. Reduction of commercial activities during the lock-down period can be argued as the major reason for the reduction in CO emissions. The places that have higher drops in NO<sub>2</sub> volumes during the confinement period have higher road, vessel and population densities. Road, vessel and population density data do not provide strong reasoning for the reduction in CO emissions due to two reasons: CO is a highly dispersing gas, and therefore, it might not be a good approach to compare the geographical location of the sensed CO gas and its sources, and people staying at home during lock-down could have created events that have both positive and negative effects on changes in CO emission levels.

## References

- [1] Agency., E.E.: Emissions of the main air pollutants in europe. <https://www.eea.europa.eu/data-and-maps/indicators/main-anthropogenic-air-pollutant-emissions/assessment-6>, accessed: 2020-10-08
- [2] Agency., E.E.: Air pollution goes down as europe takes hard measures to combat coronavirus. (2020)
- [3] Agency., E.S.: Air pollution remains low as europeans stay at home. [https://www.esa.int/Applications/Observing\\_the\\_Earth/Copernicus/Sentinel-5P/Air\\_pollution\\_remains\\_low\\_as\\_Europeans\\_stay\\_at\\_home](https://www.esa.int/Applications/Observing_the_Earth/Copernicus/Sentinel-5P/Air_pollution_remains_low_as_Europeans_stay_at_home), accessed: 2020-10-04
- [4] Agency., E.S.: Tropomi level 2, carbon monoxide total column products. version 01; copernicus sentinel-5p (processed by esa). <https://doi.org/10.5270/S5P-1hkP7rp> (2018)
- [5] Agency., E.S.: Tropomi level 2, nitrogen dioxide total column products. version 01; copernicus sentinel-5p (processed by esa). <https://doi.org/10.5270/S5P-s41jg54> (2018)
- [6] Chen, J., Jönsson, P., Tamura, M., Gu, Z., Matsushita, B., Eklundh, L.: A simple method for reconstructing a high-quality ndvi time-series data set based on the savitzky-golay filter. *Remote sensing of Environment* **91**(3-4), 332–344 (2004)
- [7] contributors., O.S.M.: Data file from "geofabrik download server" 2020; europe, 31.05.2020, data up to 2020-05-30t10:59:02z. <https://download.geofabrik.de/europe.html> (2015)
- [8] contributors., O.W.: Osmconvert. <https://wiki.openstreetmap.org/w/index.php?title=Osmconvert&oldid=1920339>, accessed: 2020-05-02
- [9] Developers., G.E.E.: Gpwv411: Population density (gridded population of the world version 4.11). [https://developers.google.com/earth-engine/datasets/catalog/CIESIN\\_GPWv411\\_GPW\\_Basic\\_Demographic\\_Characteristics](https://developers.google.com/earth-engine/datasets/catalog/CIESIN_GPWv411_GPW_Basic_Demographic_Characteristics) (2020), accessed: 2020-05-05
- [10] Go.nature.com.: Airborne nitrogen dioxide plummets over china. <https://go.nature.com/2Vxj3oQ>, accessed: 2020-10-03
- [11] Greenfacts.org.: primary and secondary pollutant. <https://www.greenfacts.org/glossary/pqrs/primary-pollutant-secondary-pollutant.htm> (2020), accessed: 2020-10-12
- [12] Iia.cnr.it.: Mobilatoria 2020 | iia.cnr.it. <http://www.iaa.cnr.it/mobilatoria-2020/>, accessed: 2020-10-08
- [13] Jenkins, N., Parfitt, H., Nicholls, M., Beckett, P., Wyche, K., Smallbone, K., Gregg, D., Smith, M.: Estimation of changes in air pollution emissions, concentrations and exposure during the covid-19 outbreak in the uk: Report for the air quality expert group, on behalf of defra: Analysis of air quality changes experienced in sussex and surrey since the covid-19 outbreak. (2020)
- [14] Le Quéré, C., J.R.J.M.S.A.A.S.A.R.D.G.A.W.D.S.Y.C.J., Friedlingstein, P.: Temporary reduction in daily global co2 emissions during the covid-19 forced confinement. *Nature Climate Change* pp. 1–7 (2020)
- [15] Mahaarachchi, B.: Analysing the change in airborne no2 and co emissions in europe during covid-19 crisis (07 2020), report prepared as the final deliverable of 'Big Data Analytics Course.'
- [16] Marinevesseltraffic.com.: Seas marine traffic - live maps | marine vessel traffic. <https://www.marinevesseltraffic.com//regions/seas> (2020), accessed: 2020-10-10
- [17] Menut, L., Bessagnet, B., Siour, G., Mailler, S., Pennel, R., Cholakian, A.: Impact of lockdown measures to combat covid-19 on air quality over western europe. *Science of the Total Environment* **741**, 140426 (2020)
- [18] MESICK, H.H.: Foliage plants for indoor removal of the primary combustion gases carbon monoxide and nitrogen dioxide. *Journal of the Mississippi Academy of Sciences* **30** (1985)
- [19] Ortiz, A.: Air quality in europe-2019 report. European Environment Agency, Luxembourg (2019)
- [20] Palisades, N.N.S.D., (SEDAC)., A.C.: Center for international earth science information network-ciesin-columbia university. 2018. gridded population of the world, version 4 (gpwv4): Population density adjusted to match 2015 revision un wpp country totals, revision 11. <https://doi.org/10.7927/H4F47M65>, accessed: 2020-03-28
- [21] RATA, V., GASPAROTTI, C., RUSU, L.: The importance of the reduction of air pollution in the black sea basin. *Mechanical Testing & Diagnosis* (2) (2017)
- [22] Sohrabi, C., Alsafi, Z., O'Neill, N., Khan, M., Kerwan, A., Al-Jabir, A., Iosifidis, C., Agha, R.: World health organization declares global emergency: A review of the 2019 novel coronavirus (covid-19). *International Journal of Surgery* (2020)

- [23] Syakila, A., Kroese, C.: The global nitrous oxide budget revisited. *Greenhouse gas measurement and management* 1(1), 17–26 (2011)
- [24] Thomas Greiner, D.o.A., University, B.E.I.S.: Carbon monoxide poisoning: Health effects. [https://www.abe.iastate.edu/extension-and-outreach/carbon-monoxide-poisoning-health-effects-aen-166/#:~:text=Carbon%20monoxide%20\(CO\)%20is%20a,spreads%20throughout%20an%20entire%20house.](https://www.abe.iastate.edu/extension-and-outreach/carbon-monoxide-poisoning-health-effects-aen-166/#:~:text=Carbon%20monoxide%20(CO)%20is%20a,spreads%20throughout%20an%20entire%20house.) (1996), accessed: 2020-10-12
- [25] Union/ESA/Copernicus, European, S.P.D., Engine., G.E.: Sentinel-5p nrti no2: Near real-time carbon monoxide., google developers. [https://developers.google.com/earth-engine/datasets/catalog/COPERNICUS\\_S5P\\_NRTI\\_L3\\_CO](https://developers.google.com/earth-engine/datasets/catalog/COPERNICUS_S5P_NRTI_L3_CO) (2020), accessed: 2020-03-10
- [26] Union/ESA/Copernicus, European, S.P.D., Engine., G.E.: Sentinel-5p nrti no2: Near real-time nitrogen dioxide., google developers. [https://developers.google.com/earth-engine/datasets/catalog/COPERNICUS\\_S5P\\_NRTI\\_L3\\_N02](https://developers.google.com/earth-engine/datasets/catalog/COPERNICUS_S5P_NRTI_L3_N02) (2020), accessed: 2020-03-20
- [27] Wiki.openstreetmap.org.: Marine navigation. [https://wiki.openstreetmap.org/wiki/Marine\\_navigation](https://wiki.openstreetmap.org/wiki/Marine_navigation) (2020), accessed: 2020-05-18
- [28] Wilbur, S., Williams, M., Williams, R., Scinicariello, F., Klotzbach, J.M., Diamond, G.L., Citra, M.: Toxicological profile for carbon monoxide. (2012)

## .1 APPENDIX

### Population density map

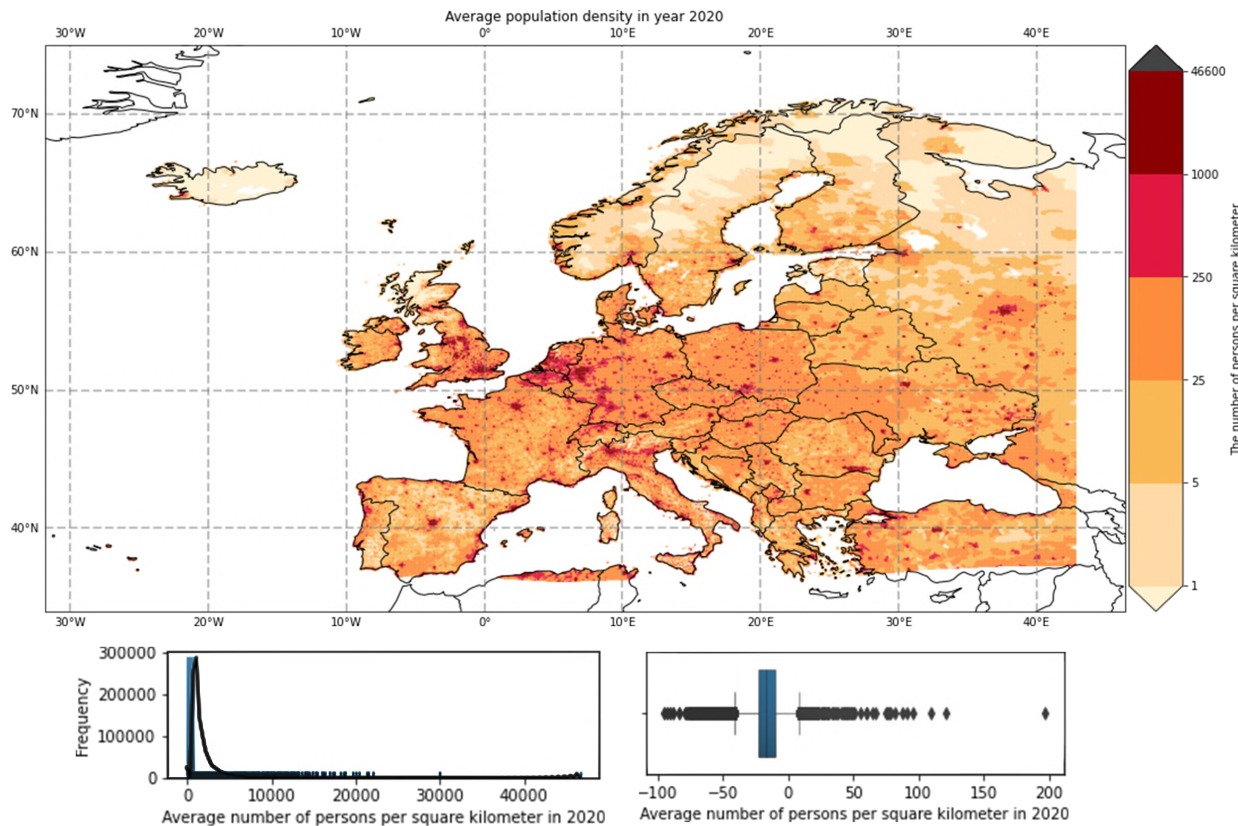


Figure .1: Estimated average number of persons for square kilometer in 2020 in Europe